

This is the Accepted Author Manuscript of the following publication:

Varrone A, Oikonen V, Forsberg A, Joutsa J, Takano A, Solin O, Haaparanta-Solin M, Nag S, Nakao R, Al-Tawil N, Wells LA, Rabiner EA, Valencia R, Schultze-Mosgau M, Thiele A, Vollmer S, Dyrks T, Lehmann L, Heinrich T, Hoffmann A, Nordberg A, Halldin C, Rinne JO. Positron emission tomography imaging of the 18-kDa translocator protein (TSPO) with [¹⁸F]FEMPA in Alzheimer's disease patients and control subjects. Eur J Nucl Med Mol Imaging. 2014 Nov 21. Doi: 10.1007/s00259-014-2955-8

The final publication is available at

<http://link.springer.com/article/10.1007%2Fs00259-014-2955-8>

European Journal of Nuclear Medicine and Molecular Imaging
Positron emission tomography imaging of the 18-kDa Translocator Protein (TSPO) with
[¹⁸F]FEMPA in Alzheimer's disease patients and control subjects
 --Manuscript Draft--

Manuscript Number:	EJNM-D-14-00503R1
Full Title:	Positron emission tomography imaging of the 18-kDa Translocator Protein (TSPO) with [¹⁸ F]FEMPA in Alzheimer's disease patients and control subjects
Article Type:	Original Article
Corresponding Author:	Andrea Varrone, M.D., Ph.D. Karolinska Institutet Stockholm, SWEDEN
Corresponding Author Secondary Information:	
Corresponding Author's Institution:	Karolinska Institutet
Corresponding Author's Secondary Institution:	
First Author:	Andrea Varrone, M.D., Ph.D.
First Author Secondary Information:	
Order of Authors:	Andrea Varrone, M.D., Ph.D.
	Vesa Oikonen
	Anton Forsberg
	Juho Joutsa
	Akihiro Takano
	Olof Solin
	Merja Haaparanta-Solin
	Sangram Nag
	Ryujia Nakao
	Nabil Al-Tawil
	Lisa A Wells
	Eugenii A Rabiner
	Ray Valencia
	Marcus Schultze-Mosgau
	Andrea Thiele
	Sonja Vollmer
	Thomas Dyrks
	Lutz Lehman
	Tobias Heinrich
	Anja Hoffmann
	Agneta Nordberg
	Christer Halldin
	Juha O Rinne

Order of Authors Secondary Information:	
Abstract:	<p>Imaging of the 18-kDa translocator protein (TSPO) is a potential tool for examining microglia activation and neuroinflammation in early Alzheimer’s disease (AD). [¹⁸F]FEMPA is a novel high-affinity, second-generation, TSPO radioligand displaying suitable pharmacokinetic properties in pre-clinical studies. The aims of this study were to assess the quantification of the binding of [¹⁸F]FEMPA to TSPO in AD patients and controls and to investigate whether higher [¹⁸F]FEMPA binding in AD vs. controls could be detected in vivo.</p> <p>Methods. Ten AD patients (5M/5F, age 66.9±7.3 y, MMSE 25.5±2.5) and seven controls (3M/4F, age 63.7±7.2 y, MMSE 29.3±1.0) were studied using [¹⁸F]FEMPA at Turku (n=13) and at Karolinska Institutet (n=4). The in vitro binding affinity for TSPO was assessed using PBR28 in a competition assay with [3H]PK11195 in 7 controls and 8 AD. Cortical and subcortical regions-of-interest were examined. Quantification was performed using two-tissue compartment model (2TCM) and Logan graphical analysis (GA). The outcome measure was the total distribution volume (VT). Repeated-measure analysis of variance was used to assess the effect of group or TSPO binding status on VT.</p> <p>Results. Five AD and 4 controls were high-affinity binders (HABs). Three AD and 3 controls were mixed-affinity binders. VT estimated with Logan GA correlated significantly with VT estimated with 2TCM in both controls (r=0.97) and AD patients (r=0.98) and was selected for the final analysis. In the medial temporal cortex, statistically significant higher VT (p=0.044) in AD vs. controls was found if the TSPO binding status was entered as covariate. If only HABs were included, statistically significant higher VT in AD patients vs. control subjects (p<0.05) was found in the medial and lateral temporal cortex, posterior cingulate, caudate, putamen, thalamus, and cerebellum.</p> <p>Conclusions. [¹⁸F]FEMPA seems to be a suitable radioligand to detect increased TSPO binding in AD if the binding status is taken into account.</p>
Response to Reviewers:	See Attachment for Reply to Reviewers.

We thank the Reviewers for the constructive and fruitful comments that helped improving the quality of the manuscript. Below is a point-by-point reply to the Reviewers' comments.

Reviewers' comments:

Reviewer #1: This is a well-designed and executed small trial of the TSPO PET tracer 18F-FEMPA in Alzheimer's disease subjects and controls. The trial was conducted at two PET centers examining 10 AD subjects and 7 controls characterized with regard to rs6971 polymorphism. A volume of interest analysis was utilized for assessing cortical and subcortical regions and data were modeled using a two tissue compartment model and a Logan graphical analysis with the primary outcome measure being total distribution volume (VT). A number of comments and questions for the authors follow:

1. The majority of the images were scanned at Turku on an ECAT EXACT HR+, while the remainder were imaged on the lower resolution ECAT EXACT HR PET tomograph. What efforts were made to standardize the reconstruction and post hoc processing of the PET data across the two sites? Were there phantoms or other analyses done to ensure the poolability of the quantitative data?

The following sentence has been included in the text to address this comment “A NEMA Jaszack phantom with spheres of different diameter and uniform background filled with 18F-radioactive solution at a ratio of ~4:1 was acquired at both centers under similar experimental conditions and using the standard reconstruction method at each centre. The difference of the recovery coefficient between the two PET systems was 9.4% for the spheres and 4.2 for the background, suggesting the possibility to pool the data from the two PET systems.” The table with the data is presented below for reviewer's perusal. We added the above sentence in the manuscript to clarify the issue.

NEMA Jaszack phantom

Diameter (mm)	9	12	15	17	25	32	
Karolinska							
RCHot	45	48.4	53.4	61.3	64.2	63.3	
RCBkg	85.2	86.7	85.9	86.8	86.2	86.3	
Turku							
RCHot	40.6	48.1	57.8	64.1	74.5	76.9	
RCBkg	93.1	87.7	83.9	80.5	89.8	88.6	
% difference (Turku-KI)/Turku							Mean % difference
RCHot	10.8	0.6	7.7	4.4	13.8	17.7	9.2
RCBkg	8.5	1.1	2.3	7.8	4.0	2.6	4.4

RC = recovery coefficient

2. The distribution of focally increased radiotracer uptake occurring with neuroinflammation may not necessarily follow boundaries of typical VOIs derived from standardized templates. Was this the case in the present investigation? If so, did the authors consider a voxel-wise analysis as an alternative to volume of interest sampling? If not, a comment to that effect in the manuscript would be useful.

This is a good point of the reviewer. However, due to the small sample size and to prevent possible type I or II errors we decided not to perform voxel-based analysis.

3. Was there correlation between regional V_T and any clinical measures?

In the text we included a new section “Additional considerations” that address this and other comments from both reviewers:

Additional considerations

The binding of [^{11}C]PBR28 to the TSPO has been shown to negatively correlate with the MMSE [19]. We examined the correlation of [^{18}F]FEMPA mean cortical (frontal, temporal, parietal, and occipital), limbic (medial temporal cortex and posterior cingulate) and sub-cortical (caudate, putamen and thalamus) V_T with MMSE and found a weak, non significant negative correlation (r between -0.37 and -0.41, p -value between 0.12 and 0.17) when combining data from controls and AD patients (data not shown), The lack of statistically significant correlation might be related to the limited sample size and further studies are needed to specifically examine the relationship between TSPO binding of [^{18}F]FEMPA and cognitive function in AD.

The analysis of the PET data was conducted using only conventional ROI-based approach. Voxel-based analysis could be useful to identify differences in small areas that can be underestimated by the use of large ROIs. In this study we did not apply voxel-based analysis because of the limited sample size of both groups and to avoid possible false-positive and negative results that can be associated with small samples.

The potential application of an ^{18}F -labelled tracer in the clinical setting could be aided by the use of a simplified acquisition protocol. However, in the case of [^{18}F]FEMPA, because of the lack of a reference region in the brain the arterial input function data is needed to estimate V_T . We did not observe differences in the parent fraction between AD patients and controls, suggesting that the observed differences in V_T are indeed reflecting differences in the brain distribution of the tracer. Such differences could be detected only by measuring the brain uptake as SUV. We did observe differences in SUV between the two groups, similar to differences in V_T (data not shown), which might suggest that SUV could be used as surrogate outcome measure. However, to validate SUV as potential outcome measure in the clinical setting, additional studies with [^{18}F]FEMPA in a larger group of AD patients and controls are needed.

4. What is the reason for the relatively poor discrimination between AD and control subjects who were mixed affinity binders, is this simply a function of signal to noise? Were the regions selected in figure 5 the "best" regions with regard to discrimination between the cohorts?

The worse discrimination between AD and control subjects in MABs can be due to the noise of the data as the reviewer noted but also on the small number of patients. The two regions presented in figure 5 were the most representative. However, all regions are presented in the Supplementary Figure.

5. The authors note a number of second generation TSPO PET radiopharmaceuticals are available. The discussion touches on some of the favorable characteristics of ^{18}F -FEMPA, but would benefit from additional information comparing the relative merits of this TSPO agent with others like ^{11}C -PBR28.

We have modified the text in the Introduction and included the following sentence to address this comment. “Based on these initial pre-clinical findings suggesting favorable kinetic properties of [^{18}F]FEMPA, it was decided to move forward with the characterization of the radioligand in human subjects. [^{18}F]FEMPA was considered to be a potential ^{18}F -labelled TSPO radioligand with similar properties (rapid wash-out from the brain and high target-to-background ratio) as the ^{11}C -labelled TSPO tracer PBR28. The aims of the present study were therefore to assess the quantification of the in vivo binding of [^{18}F]FEMPA to TSPO in AD patients and controls and to investigate whether in AD patients increased binding of [^{18}F]FEMPA to the TSPO could be demonstrated in vivo.

6. Based on these data, can the authors suggest a simplified acquisition protocol which might be suitable to clinical interrogation of neuroinflammation?

A simplified acquisition protocol cannot be easily suggested because of the need of arterial input function. Since there is no reference region in the brain for TSPO, the use of SUVratio values cannot be recommended. We did not find any obvious difference in the parent fraction, so in principle SUV data could be used, but this would require a larger number of patients and controls to confirm the findings and compare the differences between groups of V_T and SUV.

Reviewer #2: The purpose of this study was to assess the quantification of the binding of a novel high-affinity, second-generation, TSPO radioligand, [^{18}F]FEMPA, in AD patients and controls and to investigate whether higher [^{18}F]FEMPA binding in AD vs. controls could be detected in vivo.

The topic is relevant and by now few PET studies have explored TSPO imaging. None with this new ligand.

Some issues need to be addressed.

Page(P) 5 Line (L) 13 I would suggest some more recent review article like <http://www.ncbi.nlm.nih.gov/pubmed/22315714>

The reference has been changed following the recommendation of the reviewer.

P7 L49 AD was diagnosed according (NINCDS-ADRDA) and the criteria of the Diagnostic and Statistical Manual of Mental Disorders (DSM IV). Did the patients satisfy also the updated criteria for probable Alzheimer's disease dementia with evidence of the Alzheimer's disease pathophysiological process (McKhann et al., 2011) or DSM V criteria? This is important because some cases of AD (AD2, AD3, AD9) have MMSE values of 28-29.

The patients with high MMSE had probable Alzheimer's disease dementia with evidence of the Alzheimer's disease pathophysiological process (McKhann et al., 2011). In particular, AD2 had positive biomarker evidence as presence of hippocampal atrophy and reduced beta-amyloid in CSF, and AD3 had hippocampal atrophy in MRI, reduced beta-amyloid and increased tau and phosphotau in CSF. AD8 was diagnosed according to criteria of NINCDS-

ADRDA and McKann et al. 1984, neuropsychology, imaging and clinical data. AD9 was diagnosed according to the criteria of McKann et al. 2011 (pathological CSF, as well as neuropsychology data in agreement with AD).

We have included the following sentence in the text to address this comment: “In addition to these criteria, the diagnostic criteria defined by McKahn et al. that include imaging (1998) or CSF and in vivo biomarkers (2003) were used, particularly for those patients showing unimpaired global cognition (MMSE 28, 29 and 30).”

P11 L01 Why did the authors use RM-ANOVA to test the effect of the group (patients versus controls) and the TSPO binding status? The statistical design seems not to be repeated measures. A two-way ANOVA would probably be more appropriate.

As stated in the manuscript: “Repeated measure analysis of variance (RM-ANOVA) was applied to test the effect of the group (AD patients vs. controls) and TSPO binding status (MAB or HAB) on V_T . Brain region (VOI) was entered as within subject factor, the group as between subject factor and the TSPO binding status as covariate. RM-ANOVA was also applied only to the data from the HABs. In this case, no covariate was entered in the model. As post-hoc analysis, ANOVA was applied to test the differences in V_T between AD patients and controls in different brain regions.” So in principle, the statistical design was applied as a two-way ANOVA.

P13 L26 The description of the results of the RM-ANOVA seems rather to be the description of a two-way ANOVA.

See reply above.

P14 L02 This paragraph should be transposed into the 'Results' section maintaining here only the discussion of the results.

This has been done as suggested by the Reviewer.

P15 L36 The following part is too much speculative.

The reason why we included this part in the manuscript is to try to describe the results in a more comprehensive way and to try to estimate the binding potential of [^{18}F]FEMPA to provide the reader a means to compare the tracer with [^{11}C]PBR28. A similar approach has been used for [^{11}C]PBR28 by Kreisl et al. (Journal of Cerebral Blood Flow & Metabolism (2013) 33, 53–58;), providing an estimate of BP_{ND} for the HABs similar to the one of [^{18}F]FEMPA (see pages 56 and 57). Interestingly, the estimated BP_{ND} of [^{18}F]FEMPA we obtained for HABs and MABs was in agreement with the calculated BP_{ND} for [^{11}C]PBR28 recently reported by Owen et al. (Journal of Cerebral Blood Flow & Metabolism 2014; 34, 989–994) in a blocking study using the TSPO agonist XBD173. This sentence has been now included in the Discussion for clarification.

Positron emission tomography imaging of the 18-kDa Translocator Protein (TSPO) with [¹⁸F]FEMPA in Alzheimer's disease patients and control subjects

Andrea Varrone^{1*}, Vesa Oikonen^{2*}, Anton Forsberg¹, Juho Joutsa², Akihiro Takano¹, Olof Solin², Merja Haaparanta-Solin², Sangram Nag¹, Ryuji Nakao¹, Nabil Al-Tawil³, Lisa A. Wells⁴, Eugenio A. Rabiner⁴, Ray Valencia⁵, Marcus Schultze-Mosgau⁵, Andrea Thiele⁵, Sonja Vollmer⁵, Thomas Dyrks⁵, Lutz Lehman⁵, Tobias Heinrich⁵, Anja Hoffmann⁵, Agneta Nordberg⁶, Christer Halldin¹, Juha O. Rinne²

¹Karolinska Institutet, Department of Clinical Neuroscience, Centre for Psychiatry Research, Stockholm, SWEDEN

²Turku PET Centre, University of Turku, Turku, FINLAND

³Karolinska Trial Alliance, Karolinska University Hospital, Stockholm, SWEDEN

⁴Imanova Center for Imaging Sciences, London, UK

⁵Bayer Healthcare AG, Berlin, GERMANY

⁶Department of Geriatric Medicine, Karolinska University Hospital Huddinge, Stockholm, SWEDEN

*These authors equally contributed to the manuscript

Word count abstract/text: 300/4930

Financial support: Bayer Healthcare, Berlin, Germany; FP7/2007-2013-n° HEALTH-F2-2011-278850 (INMIND).

Address for correspondence:

Andrea Varrone, MD, PhD

Karolinska Institutet

Department of Clinical Neuroscience

Centre for Psychiatry Research

Karolinska Hospital R5:02

SE-17176 Stockholm, Sweden

E-mail: andrea.varrone@ki.se

1
2
3
4
5
6
7
8
9
10
11
12
13
14
15
16
17
18
19
20
21
22
23
24
25
26
27
28
29
30
31
32
33
34
35
36
37
38
39
40
41
42
43
44
45
46
47
48
49
50
51
52
53
54
55
56
57
58
59
60
61
62
63
64
65

Abstract

1
2
3 Imaging of the 18-kDa translocator protein (TSPO) is a potential tool for examining microglia
4 activation and neuroinflammation in early Alzheimer's disease (AD). [¹⁸F]FEMPA is a novel
5 high-affinity, second-generation, TSPO radioligand displaying suitable pharmacokinetic
6
7 properties in pre-clinical studies. The aims of this study were to assess the quantification of
8 the binding of [¹⁸F]FEMPA to TSPO in AD patients and controls and to investigate whether
9
10 higher [¹⁸F]FEMPA binding in AD vs. controls could be detected *in vivo*.
11
12
13
14
15
16
17

18 **Methods.** Ten AD patients (5M/5F, age 66.9±7.3 y, MMSE 25.5±2.5) and seven controls
19 (3M/4F, age 63.7±7.2 y, MMSE 29.3±1.0) were studied using [¹⁸F]FEMPA at Turku (n=13)
20 and at Karolinska Institutet (n=4). The *in vitro* binding affinity for TSPO was assessed using
21 PBR28 in a competition assay with [³H]PK11195 in 7 controls and 8 AD. Cortical and
22 subcortical regions-of-interest were examined. Quantification was performed using two-tissue
23 compartment model (2TCM) and Logan graphical analysis (GA). The outcome measure was
24 the total distribution volume (V_T). Repeated-measure analysis of variance was used to assess
25 the effect of group or TSPO binding status on V_T .
26
27
28
29
30
31
32
33
34
35
36

37 **Results.** Five AD and 4 controls were high-affinity binders (HABs). Three AD and 3 controls
38 were mixed-affinity binders. V_T estimated with Logan GA correlated significantly with V_T
39 estimated with 2TCM in both controls ($r=0.97$) and AD patients ($r=0.98$) and was selected for
40 the final analysis. In the medial temporal cortex, statistically significant higher V_T ($p=0.044$)
41 in AD vs. controls was found if the TSPO binding status was entered as covariate. If only
42 HABs were included, statistically significant higher V_T in AD patients vs. control subjects
43 ($p<0.05$) was found in the medial and lateral temporal cortex, posterior cingulate, caudate,
44 putamen, thalamus, and cerebellum.
45
46
47
48
49
50
51
52
53
54
55
56
57
58
59
60
61
62
63
64
65

1
2 **Conclusions.** [¹⁸F]FEMPA seems to be a suitable radioligand to detect increased TSPO
3 binding in AD if the binding status is taken into account.
4
5
6
7

8
9 **Key words.** Neuroinflammation, microglia, translocator protein, dementia, Alzheimer
10
11
12
13
14
15
16
17
18
19
20
21
22
23
24
25
26
27
28
29
30
31
32
33
34
35
36
37
38
39
40
41
42
43
44
45
46
47
48
49
50
51
52
53
54
55
56
57
58
59
60
61
62
63
64
65

Introduction

1
2
3 Neuroinflammation is a pathological phenomenon characterized by microglia activation
4 and reactive astrocytosis. Neuroinflammatory changes are observed in various
5
6 neurodegenerative disorders including Alzheimer's disease (AD). Post-mortem studies in AD
7
8 patients have shown that microglial activation is associated with the presence of amyloid
9
10 plaques [1], suggesting a link between amyloid pathology and neuroinflammation. In vivo
11
12 imaging of microglial activation can be a useful tool for early detection of neuroinflammation
13
14 in AD. The 18-kD translocator protein (TSPO) is a mitochondrial protein [2, 3] expressed in
15
16 macrophages [4], microglia cells [5] and reactive astrocytes [6] and is considered a marker of
17
18 activated microglia and macrophages [7]. ((*R*)-1-(2-chlorophenyl)-*N*-¹¹C-methyl-*N*-(1-
19
20 methylpropyl)-3-isoquinoline carboxamide ([¹¹C](*R*)-PK11195) was the first TSPO radioligand
21
22 developed for imaging of activated microglia. The first evidence of increased TSPO binding
23
24 in AD patients using [¹¹C](*R*)-PK11195 was reported by Cagnin et al. [8]. This finding was
25
26 replicated in a group of 13 AD patients that were also examined with the amyloid radioligand
27
28 [¹¹C]PIB [9]. A large overlap of TSPO binding signal was however observed between controls
29
30 and patients with AD or with mild cognitive impairment (MCI), using [¹¹C](*R*)-PK11195 [10,
31
32 11]. It was suggested that either microglia activation in AD is a subtle phenomenon [11] or
33
34 that [¹¹C](*R*)-PK11195 is not enough sensitive to detect in vivo increased microglia activation
35
36 in AD [10].

37
38 Several TSPO radioligands with greater affinity than [¹¹C](*R*)-PK11195 have been
39
40 developed [12] and some of them have been used for in vivo imaging of neuroinflammation.
41
42 Increased TSPO binding in AD and MCI patients compared with controls has been found
43
44 using the high-affinity radioligand *N*-(2,5-¹¹C-dimethoxybenzyl)-*N*-(5-fluoro-2-
45
46 phenoxyphenyl)acetamide ([¹¹C]DAA1106) [13, 14]. When the ¹⁸F-analog of DAA1106, *N*-
47
48

1 (5-fluoro-2-phenoxyphenyl)-*N*-(2-¹⁸F-fluoroethyl-5-methoxybenzyl)acetamide
2 ([¹⁸F]FEDAA1106) was used, no statistically significant increase of TSPO binding in AD
3 patients could be detected in comparison with controls [15]. A large variability of outcome
4 measures of [¹⁸F]FEDAA1106 among different subjects was observed [15].
5
6
7
8
9

10 A major source of variability in TSPO binding is known to be related to the presence of
11 different binding affinity profiles. This property was first demonstrated and fully examined for
12 the high-affinity TSPO radioligand (*N*-{[2-(methoxyloxy)phenyl]methyl}-*N*-[4-(phenoxy)-3-
13 pyridinyl]acetamide (PBR28) [16], but it was also shown for other second-generation TSPO
14 ligands [17]. In the case of [¹¹C]PBR28 it has been demonstrated that the *rs6971*
15 polymorphism of the TSPO gene is responsible for the presence of different binding affinity
16 profiles [18]. Subjects can be high- mixed- and low-affinity binders (HABs, MABs, LABs)
17 based on the homozygosity or heterozygosity for the polymorphism. Therefore, imaging of
18 the TSPO using second-generation radioligands should take into account the binding status of
19 the study participants, particularly when different groups of subjects are examined. Recently,
20 increased TSPO binding in amyloid-positive AD patients has been demonstrated using ¹¹C-
21 PBR28 and adjusting for TSPO genotype [19].
22
23
24
25
26
27
28
29
30
31
32
33
34
35
36
37
38
39

40 *N*-{2-[2-(¹⁸F)fluoroethoxy]-5-methoxybenzyl}-*N*-[2-(4-methoxyphenoxy)pyridine-3-
41 yl]acetamide ([¹⁸F]FEMPA [CAS 1207345-42-3]) is an aryloxyipyridylamide derivative that is
42 less lipophilic than [¹⁸F]FEDAA1106, and pre-clinical data in non-human primates showed a
43 fast elimination from the brain and a better signal-to-noise ratio. Based on these initial pre-
44 clinical findings suggesting favorable kinetic properties of [¹⁸F]FEMPA, it was decided to
45 move forward with the characterization of the radioligand in human subjects. [¹⁸F]FEMPA
46 was considered to be a potential ¹⁸F-labelled TSPO radioligand with similar kinetic properties
47 (rapid wash-out from the brain and high target-to-background ratio) as the ¹¹C-labelled TSPO
48
49
50
51
52
53
54
55
56
57
58
59
60
61
62
63
64
65

1 tracer PBR28. The aims of the present study were therefore to assess the quantification of the
2 in vivo binding of [¹⁸F]FEMPA to TSPO in AD patients and controls and to investigate
3
4 whether in AD patients increased binding of [¹⁸F]FEMPA to the TSPO could be demonstrated
5
6
7 in vivo.
8
9

10
11
12
13
14
15
16
17
18
19
20
21
22
23
24
25
26
27
28
29
30
31
32
33
34
35
36
37
38
39
40
41
42
43
44
45
46
47
48
49
50
51
52
53
54
55
56
57
58
59
60
61
62
63
64
65

Materials and methods

Subjects

The study was conducted in line with the Helsinki Declaration and approved by FIMEA and the Swedish Medical Products Agency, the local Ethics Committee of the Southwest Hospital District of Finland and of the Stockholm region, and by the Radiation Safety Committee of the Turku Hospital and the Karolinska University Hospital. The study was registered at www.ClinicalTrials.gov (NCT01153607) and included a total of 24 participants. Seventeen of those participants were included in the present study, whereas 7 participants were included in a whole-body dosimetry study that will be reported separately.

Ten AD patients and 7 controls were studied at Turku PET Centre (13 subjects) and at Karolinska Institutet (4 subjects) (Table 1). All subjects gave written informed consent for participation in the study. AD patients were recruited from the University of Turku and from the Karolinska University Hospital, Huddinge. Controls were recruited by local advertisement and from a database at the Karolinska Trial Alliance in Stockholm. All subjects underwent careful clinical and neurological examinations, Mini-Mental State Examination (MMSE), and neuropsychological testing including assessment of memory function. Probable AD was diagnosed according to the clinical criteria of the National Institute of Neurological and Communicative Disorders and Stroke and Alzheimer's Disease and Related Disorders Association (NINCDS-ADRDA) and the criteria of the Diagnostic and Statistical Manual of Mental Disorders (DSM IV). In addition to these criteria, the diagnostic criteria defined by McKahn et al. that include imaging (1998) or CSF and in vivo biomarkers (2003) were used, particularly for those patients showing unimpaired global cognition (MMSE 28, 29 and 30). The inclusion criterion was mild to moderate disease (MMSE score ≥ 20 and a Clinical Dementia Rating score of 1 or 2). Other forms of dementia (e.g. dementia with Lewy bodies)

1 had to be excluded. Patients were under stable treatment (at least 6 months before the study)
2 with cholinesterase inhibitors. Additionally, neither AD patients nor controls were allowed to
3 show signs of systemic autoimmune or inflammatory disease. Participants with other current
4 treatments acting on the central nervous system (including anti-inflammatory treatments in
5 pre-specified time frames) were also excluded in order to avoid interference with the in vivo
6 binding of the radioligand.
7

14 *PET experimental procedures*

15
16
17
18
19
20
21
22
23
24
25
26
27
28
29
30
31
32
33
34
35
36
37
38
39
40
41
42
43
44
45
46
47
48
49
50
51
52
53
54
55
56
57
58
59
60
61
62
63
64
65
Details of radiolabelling procedures of [¹⁸F]FEMPA are described in Supplementary
Appendix 1. Specific radioactivity at time of injection was between 31 and 1343 GBq/μmol.
The injected radioactivity was 251±16 MBq in control subjects and 251±10 MBq in AD
patients. The injected mass was 0.68±0.97 (range 0.07-2.55) μg in control subjects and
0.67±1.16 (range 0.09-3.74) μg in AD patients. There were no significant adverse or clinically
detectable pharmacologic effects in any of the 17 subjects. No significant changes in vital
signs or the results of laboratory studies or electrocardiograms were observed.

37 *PET measurements*

40
41
42
43
44
45
46
47
48
49
50
51
52
53
54
55
56
57
58
59
60
61
62
63
64
65
PET measurements were performed with the ECAT EXACT HR+ (Turku PET Center)
and the ECAT EXACT HR (Karolinska Institutet) systems in two PET sessions. The first PET
session consisted of a 90-min dynamic acquisition with a series of frames of increasing
duration (6x5 sec, 3x10 sec, 2x20 sec, 4x60 sec, 6x180 sec, 11x360 sec). The second PET
session of 30 min was performed between 120 and 150 min after radioligand injection and
consisted of 5 frames of 360 sec. A transmission scan of 5 min was acquired before each
dynamic acquisition using three rotating ⁶⁸Ge sources. At Turku, images were reconstructed
with filtered back projection, a 256x256 matrix, and a pixel size of 1.226x1.226 mm. At

1 Karolinska Institutet, images were reconstructed with filtered back projection, with a 2-mm
2 Hanning filter, a zoom factor of 2.17, and a 128x128 matrix. Images were corrected for
3
4 attenuation and scatter. A NEMA Jaszack phantom with spheres of different diameter and
5
6 uniform background filled with ^{18}F -radioactive solution at a ratio of ~4:1 was acquired at both
7
8 centers under similar experimental conditions and using the standard reconstruction method at
9
10 each centre. The difference of the recovery coefficient between the two PET systems was
11
12 9.4% for the spheres and 4.2 for the background, suggesting the possibility to pool the data
13
14 from the two PET systems.
15
16
17
18
19

20 Arterial blood sampling was performed using an automated blood sampling system
21
22 (Allogg AB, Mariefred, Sweden) for the first 10 min and using manual samples thereafter.
23
24 Samples for metabolite analysis (HPLC, Appendix 1) were taken at 2, 5, 10.5, 20, 30, 45, 60,
25
26 90, 120, and 150 min.
27
28
29

30 *Magnetic resonance imaging*

31
32
33
34 MRI was performed at Turku University using a Philips Gyroscan Intera 1.5 T Nova
35
36 Dual scanner (Philips, Best, the Netherlands) and at the Karolinska Institutet using a 1.5-T GE
37
38 Signa system (GE Healthcare, Milwaukee, WI). MRI scans consisted of a T2-weighted
39
40 sequence for ruling out pathological changes and a 3-D T1-weighted spoiled gradient recalled
41
42 (SPGR) sequence for both coregistration with PET and volume-of-interest (VOI) analysis.
43
44 MRI scans were evaluated for white matter changes according to the Age-Related White
45
46 Matter Changes (ARWMC) scale [20], and exclusion criteria were an ARWMC score of >1 in
47
48 the basal ganglia and >2 in the subcortical white matter.
49
50
51
52
53
54
55
56
57
58
59
60
61
62
63
64
65

Image analysis

1
2
3 Image analysis was performed at Turku PET Centre. PET images were coregistered to
4
5 the T1-weighted MRI using SPM2 (Wellcome Department of Imaging Neuroscience, London,
6
7 UK). Volumes of interest (VOIs) were delineated using the software Imadeus 1.20 (Forima
8
9 Inc, Turku, Finland). The following regions were defined: frontal cortex, parietal cortex,
10
11 lateral and medial temporal cortex, occipital cortex, posterior cingulate cortex, caudate,
12
13 putamen, thalamus, pons, cerebellum and the subcortical white matter.
14
15
16
17

TSPO binding status

18
19
20
21
22 The TSPO binding status was measured at Imanova Centre for Imaging Sciences from
23
24 peripheral blood samples. In two AD patients (AD1 and AD2) the plasma was not available
25
26 for the binding competition assay. The PBR28 binding status was measured using competition
27
28 binding assay with ³H-PK11195 on platelet membrane suspension (Supplementary Appendix
29
30 2). Data were analysed using GraphPad Prism 5.0 Software. One and two site binding models
31
32 were compared using a sum-of-square *F*-test. In four subjects (CS6, CS7, AD8, and AD9), the
33
34 binding status was less reliably measured because of low protein concentration in the samples.
35
36
37
38
39

Data analysis

40
41
42
43 A preliminary analysis showed that the first PET session was sufficient for
44
45 quantification of [¹⁸F]FEMPA binding. Therefore, only 90 min of data were used for the final
46
47 analysis. The radioactivity concentration in the different brain regions was reported as
48
49 standard uptake value (SUV) and calculated as $SUV = kBq/cm^3 \div Bq \text{ injected} / \text{body weight}$
50
51 (g). Two parameters were measured to assess the kinetic properties of [¹⁸F]FEMPA: the time
52
53 to peak uptake (t_{peak}) and the time when the brain radioactivity decreased to 50% of the peak
54
55 ($t_{\text{half-peak}}$), both expressed in min. The quantification was performed using kinetic and Logan
56
57
58
59
60
61
62
63
64
65

1 graphical analysis (GA). Kinetic analysis was performed with nonlinear least square (NLS)
2 fitting and two tissue compartment model (2TCM), with four parameters (K_1 , K_1/k_2 , k_3/k_4 , k_4)
3 and blood volume fitted for each region. The outcome measure was the total distribution
4 volume (V_T). In one subject (AD2), arterial blood sampling was not successful, and this
5 patient was excluded from further analyses. The variability of V_T estimated with 2TCM and
6 Logan GA was calculated as the ratio between the SD over the mean for each brain region and
7 expressed as percentage (coefficient of variance=COV%).

17 *Statistical analysis*

18
19
20
21 Regression analysis was used to assess the agreement between 2TCM and Logan GA in
22 the estimation of V_T . F-test was used to compare the variability of V_T (%COV) estimated with
23 2TCM and Logan GA. Repeated measure analysis of variance (RM-ANOVA) was applied to
24 test the effect of the group (AD patients vs. controls) and TSPO binding status (MAB or
25 HAB) on V_T . Brain region (VOI) was entered as within subject factor, the group as between
26 subject factor and the TSPO binding status as covariate. RM-ANOVA was also applied only
27 to the data from the HABs. In this case, no covariate was entered in the model. As post-hoc
28 analysis, ANOVA was applied to test the differences in V_T between AD patients and controls
29 in different brain regions. Statistical significance was evaluated at $p < 0.05$.

Results

TSPO binding status

Four controls were HABs and 3 were MABs, whereas 5 AD patients were HABs and 3 were MABs (Supplementary Appendix 2). No LABs were observed in either group. The K_i high for the HABs was 2.26 ± 0.18 nM. The K_i high and low for the MABs were 1.93 ± 0.75 nM and 189.8 ± 14.4 nM, respectively.

Radiometabolite analysis

[^{18}F]FEMPA showed rapid metabolism in vivo with <20% of tracer present in plasma 20 min after injection and <10% after 90 min (Figure 1 and Supplementary Figure 1 and 2). There were no statistically significant differences in the parent fraction or in the fraction of metabolites between control subjects and AD patients and between MABs and HABs (Figure 1).

Kinetic properties of [^{18}F]FEMPA

Representative SUV images and mean time-activity curves of [^{18}F]FEMPA are presented in Figures 2 and 3. In each binding group there were no statistically significant differences between controls and AD patients in kinetic parameters based on SUV data (Supplementary Table 1). However, among the AD patients the $t_{\text{half-peak}}$ was significantly lower in MABs than in HABs ($p=0.008$), whereas only a trend was observed in the controls ($p=0.15$).

PET quantification

A preliminary comparison between one tissue compartment model and 2TCM showed that 2TCM provided a better fitting of the data by visual inspection and based on Akaike

1 Information Criteria, therefore only 2TCM was used in the final analysis of the data
2 (Supplementary Figure 3, Supplementary Table 2 and 3). In HABs, V_T values were
3
4 significantly higher ($p<0.05$) in AD patients compared with controls in parietal cortex, lateral
5
6 and medial temporal cortex, posterior cingulate, thalamus and cerebellum.
7
8
9

10 Representative Logan plots of [^{18}F]FEMPA are presented in Figure 4. There was a
11
12 statistically significant correlation between V_T estimated with 2TCM and with Logan GA in
13
14 controls ($r=0.97$, $p<0.001$) and AD patients ($r=0.98$, $p<0.001$) across all regions and subjects,
15
16 with values close to the line of identity (Supplementary Figure 4). The mean COV% of V_T
17
18 estimated with Logan GA tended to be lower than the mean COV% of V_T estimated with
19
20 2TCM in AD patients ($p=0.05$, Supplementary Table 4). Logan GA was selected for the final
21
22 analysis of the data, considering the high correlation of V_T between Logan GA and 2TCM and
23
24 the slightly lower COV% of V_T estimated with Logan GA in AD patients.
25
26
27
28
29

30 RM-ANOVA using Logan V_T showed a significant effect of TSPO ($F=17.3$, $p=0.001$)
31
32 and a significant region*TSPO binding status interaction ($F=5.2$, $p=0.004$). The group showed
33
34 only a non-significant trend ($F=3.7$, $p=0.077$). No statistically significant region*group
35
36 interaction was found. However, when only HABs were included in the analysis, a significant
37
38 effect of group ($F=9.2$, $p=0.02$) was observed but no statistically significant region*group
39
40 interaction was found. In all subjects, if the TSPO binding status was entered as covariate, a
41
42 statistically significant difference between groups was found in the medial temporal cortex
43
44 (Table 2). If only the HABs were included, statistically significant differences between groups
45
46 were found in lateral and medial temporal cortex, posterior cingulate, caudate, putamen,
47
48 thalamus and cerebellum (Table 2). In HABs, the V_T values (mean \pm SD) in these regions were
49
50 on average $19.5\pm 3.0\%$ higher in AD patients as compared with controls, ranging from 15%
51
52
53
54
55
56
57
58
59
60
61
62
63
64
65

higher in the lateral temporal cortex to 24% in the thalamus (Table 2, Figure 5 and
Supplementary Figure 5).

1
2
3
4
5
6
7
8
9
10
11
12
13
14
15
16
17
18
19
20
21
22
23
24
25
26
27
28
29
30
31
32
33
34
35
36
37
38
39
40
41
42
43
44
45
46
47
48
49
50
51
52
53
54
55
56
57
58
59
60
61
62
63
64
65

Discussion

This study was designed to examine the quantification of the binding to TSPO of the novel radioligand [^{18}F]FEMPA in controls and AD patients and to evaluate whether increased TSPO binding in AD could be demonstrated in vivo. The primary outcome measure in this study was V_T , estimated using kinetic and Logan GA and the metabolite corrected arterial input function, since no reference region for TSPO is present in the brain. Since a major source of variability in V_T for all second-generation TSPO radioligands is known to come from the *rs6971* polymorphism of the TSPO [18], the binding status of the subjects was evaluated using competition assay with ^3H -PK11195 and PBR28. In a separate work, the binding properties of FEMPA have been tested on human brain tissue samples, known to belong to different binder subtypes, and it was found that the ratio in affinity between LABs and HABs was approximately 12 (unpublished, data), thus ~ 4.6 times lower than PBR28.

The main finding of this study was that increased in vivo binding of [^{18}F]FEMPA to TSPO in AD patients could be demonstrated if the binding status of the subjects was taken into account and more specifically if only HABs were included. [^{18}F]FEMPA appeared to be a suitable radioligand for in vivo TSPO quantification, displaying good brain uptake, fast wash-out from the brain and relatively fast metabolism. V_T estimated using Logan GA was in very good agreement with V_T estimated using 2TCM and showed also lower variability in both controls and AD patients.

TSPO binding status

In this study the TSPO binding status was examined in a competition assay with ^3H -PK11195 and PBR28. It is known that this assay provides results in agreement with the analysis of the polymorphism of the TSPO gene [21]. The K_i high for the HABs was in good

1 agreement with the K_i value (3.10 ± 5 nM) previously reported by Owen et al. [16]. The K_i
2 high and low for the MABs were also in agreement with the K_i high and low values (4.0 ± 2.4
3 and 313 ± 76.8 nM) previously reported [16], although the K_i low for MABs was more in
4 agreement with the K_i low previously reported for LABs (188 ± 15.6 nM) [16]. Although in 4
5 subjects the protein concentration in the assay was low, leading to a reduced signal-to-noise
6 ratio, the V_T for HABs was approximately 2.2 times higher than the V_T for MABs, in
7 agreement with the ratio of V_T between HABs and MABs found across all subjects, which was
8 approximately 1.5. This ratio is also in agreement with the ratio between HABs and MABs
9 reported for ^{11}C -PBR28 [18].

22 *Quantification of [^{18}F]FEMPA binding to TSPO*

26 The fast kinetic properties of [^{18}F]FEMPA compared with its analog [^{18}F]FEDAA1106
27 represent a potential advantage for its clinical use. The kinetic analysis showed that the 2TCM
28 was a suitable model for the quantification of [^{18}F]FEMPA and that V_T estimates obtained
29 with Logan GA were in close agreement with the 2TCM. In this study, we only observed
30 HABs and MABs according to the in vitro binding affinity data. We attempted to estimate the
31 V_T for a LAB, based on the results of the MABs and HABs (Supplementary Appendix 3). The
32 estimated $V_{T\text{LAB}}$ was 0.57 ± 0.08 in controls and 0.74 ± 0.28 in AD patients. Interestingly, this
33 value is similar to the lowest V_T value found in the AD patient that was not analysed for the
34 binding status and that most likely corresponds to a LAB. Assuming that the non-specific
35 binding is similar in HABs, MABs and LABs, and that $V_{\text{ND}} < V_T^{\text{LAB}}$, the binding potential
36 (BP_{ND}) calculated from the distribution volumes ($BP_{\text{ND}} = V_T/V_{\text{ND}} - 1$) can be estimated to be at
37 least ~ 2 in HABs and ~ 1 in MABs. Interestingly, the estimated BP_{ND} of [^{18}F]FEMPA we
38 obtained for HABs and MABs was in agreement with the calculated BP_{ND} for [^{11}C]PBR28
39 recently reported by Owen et al. in a blocking study using the TSPO agonist XBD173 [22].

Increased TSPO binding in AD

We observed that in HABs the increase of [¹⁸F]FEMPA binding to the TSPO was between 15% and 24%. These findings are in agreement with previous reports using either [¹¹C](R)-PK11195 in AD patients (approximately 20-35% increased in cortical binding as compared with controls) (9), [¹¹C]DAA1106 in MCI (26% increase) and AD patients (18% increase) (13, 14), or [¹¹C]PBR28 in AD patients (38% increase) (19). Considering the relatively small sample size of this study, statistically significant increased TSPO signal in early AD was detected only after controlling for the TSPO binding status, suggesting the potential of [¹⁸F]FEMPA to detect microglia activation in AD.

Additional considerations

The binding of [¹¹C]PBR28 to the TSPO has been shown to correlate negatively with the MMSE [19]. We examined the correlation of [¹⁸F]FEMPA mean cortical (frontal, temporal, parietal, and occipital), limbic (medial temporal cortex and posterior cingulate) and sub-cortical (caudate, putamen and thalamus) V_T with MMSE and found a weak, non significant negative correlation (r between -0.37 and -0.41, p -value between 0.12 and 0.17) when combining data from controls and AD patients (data not shown). The lack of statistically significant correlation might be related to the limited sample size and further studies are needed to specifically examine the relationship between TSPO binding of [¹⁸F]FEMPA and cognitive function in AD.

The analysis of the PET data was conducted using only conventional ROI-based approach. Voxel-based analysis could be useful to identify differences in small areas that can be underestimated by the use of large ROIs. In this study we did not apply voxel-based

1 analysis because of the limited sample size of both groups and to avoid possible false-positive
2 and negative results that can be associated with small samples.
3
4

5 The potential application of an ^{18}F -labelled tracer in the clinical setting could be aided
6 by the use of a simplified acquisition protocol. However, in the case of [^{18}F]FEMPA, because
7 of the lack of a reference region in the brain the arterial input function data is needed to
8 estimate V_T . We did not observe differences in the parent fraction between AD patients and
9 controls, suggesting that the observed differences in V_T are indeed reflecting differences in the
10 brain distribution of the tracer. Such differences could be detected only by measuring the
11 brain uptake as SUV. We did observe differences in SUV between the two groups, similar to
12 differences in V_T (data not shown), which might suggest that SUV could be used as surrogate
13 outcome measure. However, to validate SUV as potential outcome measure in the clinical
14 setting, additional studies with [^{18}F]FEMPA in a larger group of AD patients and controls are
15 needed.
16
17
18
19
20
21
22
23
24
25
26
27
28
29
30
31

32 **Conclusions**

33 [^{18}F]FEMPA seems to be a suitable radioligand for in vivo imaging and quantification of
34 TSPO in early AD, provided that the TSPO binding status is determined or by including only
35 HABs. Future studies are needed to confirm these findings in a larger cohort of AD patients.
36
37
38
39
40
41
42
43

44 **Acknowledgments**

45 This study was sponsored by Bayer Healthcare, Berlin, Germany. The work at Turku
46 PET Centre and Karolinska Institutet was supported by the European Union's Seventh
47 Framework Programme (FP7/2007-2013) under grant agreement n^o HEALTH-F2-2011-
48 278850 (INMIND). The compound [^{18}F]FEMPA is now part of the portfolio of the Piramal
49 Imaging GmbH, Berlin, Germany. The authors thank the staff of the Turku PET Centre, the
50
51
52
53
54
55
56
57
58
59
60
61
62
63
64
65

Karolinska Institutet PET Centre and the Karolinska University Hospital for technical support.

1
2
3
4
5
6
7
8
9
10
11
12
13
14
15
16
17
18
19
20
21
22
23
24
25
26
27
28
29
30
31
32
33
34
35
36
37
38
39
40
41
42
43
44
45
46
47
48
49
50
51
52
53
54
55
56
57
58
59
60
61
62
63
64
65

1
2
3
4
5
6
7
8
9
10
11
12
13
14
15
16
17
18
19
20
21
22
23
24
25
26
27
28
29
30
31
32
33
34
35
36
37
38
39
40
41
42
43
44
45
46
47
48
49

Table 1. Details of Controls and AD patients and their binding status.

Controls/AD patients	Centre	Gender	Age (y)	MMSE	Binding status	Treatment
CS1	Turku	M	66	28	HAB	n.a.
CS2	Turku	F	56	29	MAB	n.a.
CS3	Turku	M	55	30	MAB	n.a.
CS4	Turku	F	69	30	HAB	n.a.
CS5	Turku	F	71	28	HAB	n.a.
CS6	KI	M	58	30	MAB	n.a.
CS7	KI	F	71	30	HAB	n.a.
Mean±SD		64±7	29.3±1.0			
AD1	Turku	M	74	23	na	Rivastigmine 9.5mg QD
AD2*	Turku	F	56	29	na	Donepezil 10mg QD
AD3	Turku	M	69	28	HAB	Rivastigmine 9.5mg QD
AD4	Turku	M	55	25	MAB	Donepezil 10mg QD
AD5	Turku	F	67	26	HAB	Rivastigmine 9.5mg QD
AD6	Turku	F	76	24	HAB	Donepezil 10mg QD
AD7	Turku	F	67	22	MAB	Donepezil 5mg QD
AD8	KI	F	71	27	HAB	Donepezil 5 mg
AD9	KI	M	61	28	MAB	Galantamine 16 mg
AD10	Turku	M	73	23	HAB	Donepezil 10 mg QD
Mean±SD		67±7	25.5±2.5†			

*AD2: not analysed because only 10 min of blood data available

†= significantly different from Controls by two-tailed un-paired t-test, $p=0.002$

HAB = High Affinity Binder (9), MAB = Mixed Affinity Binder (6), LAB = Low Affinity Binder (0).

Table 2. V_T values of Logan GA in Controls and AD patients (mean \pm SD) with results of ANOVA. The analysis was conducted on all subjects (HABs and MABs) and on the HAB subjects only (4 Controls, 5 AD patients). In the ANOVA conducted on all subjects, the TSPO binding status was included as covariate.

Region	V_T , all subjects			V_T , only HABs		
	Controls	AD patients	Group <i>F</i> (<i>p</i> value)	Controls	AD patients	Group <i>F</i> (<i>p</i> value)
Frontal cx	1.59 \pm 0.40	1.68 \pm 0.63	1.8 (0.202)	1.85 \pm 0.12	2.12 \pm 0.23	4.4 (0.075)
Parietal cx	1.40 \pm 0.32	1.61 \pm 0.52	4.6 (0.052)	1.61 \pm 0.17	1.86 \pm 0.16	5.2 (0.056)
Lat Temp cx	1.50 \pm 0.35	1.61 \pm 0.55	2.8 (0.122)	1.72 \pm 0.10	1.98 \pm 0.17	7.0 (0.033)
Med Temp cx	1.64 \pm 0.48	1.88 \pm 0.69	5.1 (0.044)	1.95 \pm 0.12	2.36 \pm 0.18	15.2 (0.006)
Occip cx	1.46 \pm 0.35	1.60 \pm 0.52	2.3 (0.154)	1.65 \pm 0.28	1.82 \pm 0.23	1.0 (0.353)
Post Cingulate	1.62 \pm 0.44	1.86 \pm 0.67	4.1 (0.066)	1.91 \pm 0.10	2.30 \pm 0.24	9.1 (0.020)
Caudate	1.25 \pm 0.33	1.35 \pm 0.49	1.9 (0.193)	1.45 \pm 0.05	1.68 \pm 0.19	6.0 (0.045)
Putamen	1.46 \pm 0.44	1.67 \pm 0.64	3.6 (0.080)	1.73 \pm 0.10	2.10 \pm 0.23	8.9 (0.020)
Thalamus	1.64 \pm 0.48	1.89 \pm 0.75	4.1 (0.064)	1.94 \pm 0.09	2.40 \pm 0.29	9.1 (0.019)
Pons	1.70 \pm 0.50	1.92 \pm 0.80	2.8 (0.121)	2.00 \pm 0.15	2.42 \pm 0.35	5.0 (0.060)
Cerebellum	1.43 \pm 0.35	1.61 \pm 0.60	4.2 (0.064)	1.67 \pm 0.06	2.00 \pm 0.24	6.9 (0.034)
White matter	1.44 \pm 0.44	1.61 \pm 0.66	2.4 (0.146)	1.70 \pm 0.14	2.03 \pm 0.33	3.3 (0.111)

Figure Legend

Figure 1. Mean plasma parent fraction in mixed-affinity binder (MAB) and high-affinity binder (HAB) in controls and AD patients. The error bars represent 1 SD.

Figure 2. Representative SUV images of mixed-affinity binders (MAB) and high-affinity binders (HAB). Transaxial slices at the level of the basal ganglia from two control subjects and two AD patients are shown. Frames between 5 and 30 min (top row) and between 60 and 90 min (bottom row) were averaged.

Figure 3. Mean TACs from mixed-affinity binder (MAB) and high-affinity binder (HAB) Controls and AD patients in thalamus and medial temporal cortex. Error bars represent 1 SD.

Figure 4. Representative Logan plots of thalamus and medial temporal cortex from mixed-affinity binders (MAB) and high-affinity binders (HAB). Data are from the same control subjects and AD patients displayed in Figure 2.

Figure 5. Scatter plot of V_T values in control subjects and AD patients (HABs and MABs) for thalamus and medial temporal cortex. The AD patient displayed with the open square was not analysed for TSPO binding.

Conflict of interest

Ray Valencia, Marcus Schultze-Mosgau, Andrea Thiele, Sonja Vollmer, Thomas Dyrks, Lutz Lehman, Tobias Heinrich, Anja Hoffmann were employed by Bayer Healthcare, Berlin, Germany at the time of the conduction of the study.

References

1. Wyss-Coray T, Rogers J. Inflammation in Alzheimer disease-a brief review of the basic science and clinical literature. *Cold Spring Harb Perspect Med.* 2012;2:a006346.
2. Rupprecht R, Papadopoulos V, Rammes G, Baghai TC, Fan J, Akula N, et al. Translocator protein (18 kDa) (TSPO) as a therapeutic target for neurological and psychiatric disorders. *Nat Rev Drug Discov.* 2010;9:971-88.
3. Scarf AM, Kassiou M. The translocator protein. *J Nucl Med.* 2011;52:677-80.
4. Bird JL, Izquierdo-Garcia D, Davies JR, Rudd JH, Probst KC, Figg N, et al. Evaluation of translocator protein quantification as a tool for characterising macrophage burden in human carotid atherosclerosis. *Atherosclerosis.* 2010;210:388-91.
5. Cosenza-Nashat M, Zhao ML, Suh HS, Morgan J, Natividad R, Morgello S, et al. Expression of the translocator protein of 18 kDa by microglia, macrophages and astrocytes based on immunohistochemical localization in abnormal human brain. *Neuropathol Appl Neurobiol.* 2009;35:306-28.
6. Kuhlmann AC, Guilarte TR. Cellular and subcellular localization of peripheral benzodiazepine receptors after trimethyltin neurotoxicity. *J Neurochem.* 2000;74:1694-704.
7. Venneti S, Lopresti BJ, Wiley CA. Molecular imaging of microglia/macrophages in the brain. *Glia.* 2012.
8. Cagnin A, Brooks DJ, Kennedy AM, Gunn RN, Myers R, Turkheimer FE, et al. In-vivo measurement of activated microglia in dementia. *Lancet.* 2001;358:461-7.
9. Edison P, Archer HA, Gerhard A, Hinz R, Pavese N, Turkheimer FE, et al. Microglia, amyloid, and cognition in Alzheimer's disease: An [11C](R)PK11195-PET and [11C]PIB-PET study. *Neurobiol Dis.* 2008;32:412-9.

- 1
2
3
4
5
6
7
8
9
10
11
12
13
14
15
16
17
18
19
20
21
22
23
24
25
26
27
28
29
30
31
32
33
34
35
36
37
38
39
40
41
42
43
44
45
46
47
48
49
50
51
52
53
54
55
56
57
58
59
60
61
62
63
64
65
10. Wiley CA, Lopresti BJ, Venetis S, Price J, Klunk WE, DeKosky ST, et al. Carbon 11-labeled Pittsburgh Compound B and carbon 11-labeled (R)-PK11195 positron emission tomographic imaging in Alzheimer disease. *Arch Neurol.* 2009;66:60-7.
 11. Schuitemaker A, Kropholler MA, Boellaard R, van der Flier WM, Kloet RW, van der Doef TF, et al. Microglial activation in Alzheimer's disease: an (R)-[(1)(1)C]PK11195 positron emission tomography study. *Neurobiol Aging.* 2013;34:128-36.
 12. Dolle F, Luus C, Reynolds A, Kassiou M. Radiolabelled molecules for imaging the translocator protein (18 kDa) using positron emission tomography. *Curr Med Chem.* 2009;16:2899-923.
 13. Yasuno F, Ota M, Kosaka J, Ito H, Higuchi M, Doronbekov TK, et al. Increased binding of peripheral benzodiazepine receptor in Alzheimer's disease measured by positron emission tomography with [11C]DAA1106. *Biol Psychiatry.* 2008;64:835-41.
 14. Yasuno F, Kosaka J, Ota M, Higuchi M, Ito H, Fujimura Y, et al. Increased binding of peripheral benzodiazepine receptor in mild cognitive impairment-dementia converters measured by positron emission tomography with [(1)(1)C]DAA1106. *Psychiatry Res.* 2012;203:67-74.
 15. Varrone A, Mattsson P, Forsberg A, Takano A, Nag S, Gulyas B, et al. In vivo imaging of the 18-kDa translocator protein (TSPO) with [18F]FEDAA1106 and PET does not show increased binding in Alzheimer's disease patients. *Eur J Nucl Med Mol Imaging.* 2013;40:921-31.
 16. Owen DR, Howell OW, Tang SP, Wells LA, Bennacef I, Bergstrom M, et al. Two binding sites for [3H]PBR28 in human brain: implications for TSPO PET imaging of neuroinflammation. *J Cereb Blood Flow Metab.* 2010;30:1608-18.

- 1
2
3
4
5
6
7
8
9
10
11
12
13
14
15
16
17
18
19
20
21
22
23
24
25
26
27
28
29
30
31
32
33
34
35
36
37
38
39
40
41
42
43
44
45
46
47
48
49
50
51
52
53
54
55
56
57
58
59
60
61
62
63
64
65
17. Owen DR, Gunn RN, Rabiner EA, Bennacef I, Fujita M, Kreisl WC, et al. Mixed-affinity binding in humans with 18-kDa translocator protein ligands. *J Nucl Med.* 2011;52:24-32.
 18. Owen DR, Yeo AJ, Gunn RN, Song K, Wadsworth G, Lewis A, et al. An 18-kDa translocator protein (TSPO) polymorphism explains differences in binding affinity of the PET radioligand PBR28. *J Cereb Blood Flow Metab.* 2012;32:1-5.
 19. Kreisl WC, Lyoo CH, McGwier M, Snow J, Jenko KJ, Kimura N, et al. In vivo radioligand binding to translocator protein correlates with severity of Alzheimer's disease. *Brain.* 2013;136:2228-38.
 20. Wahlund LO, Barkhof F, Fazekas F, Bronge L, Augustin M, Sjogren M, et al. A new rating scale for age-related white matter changes applicable to MRI and CT. *Stroke.* 2001;32:1318-22.
 21. Kreisl WC, Jenko KJ, Hines CS, Lyoo CH, Corona W, Morse CL, et al. A genetic polymorphism for translocator protein 18 kDa affects both in vitro and in vivo radioligand binding in human brain to this putative biomarker of neuroinflammation. *J Cereb Blood Flow Metab.* 2013;33:53-8.
 22. Owen DR, Guo Q, Kalk NJ, Colasanti A, Kalogiannopoulou D, Dimber R, et al. Determination of [(11)C]PBR28 binding potential in vivo: a first human TSPO blocking study. *J Cereb Blood Flow Metab.* 2014;34:989-94.

Figure 1
[Click here to download high resolution image](#)

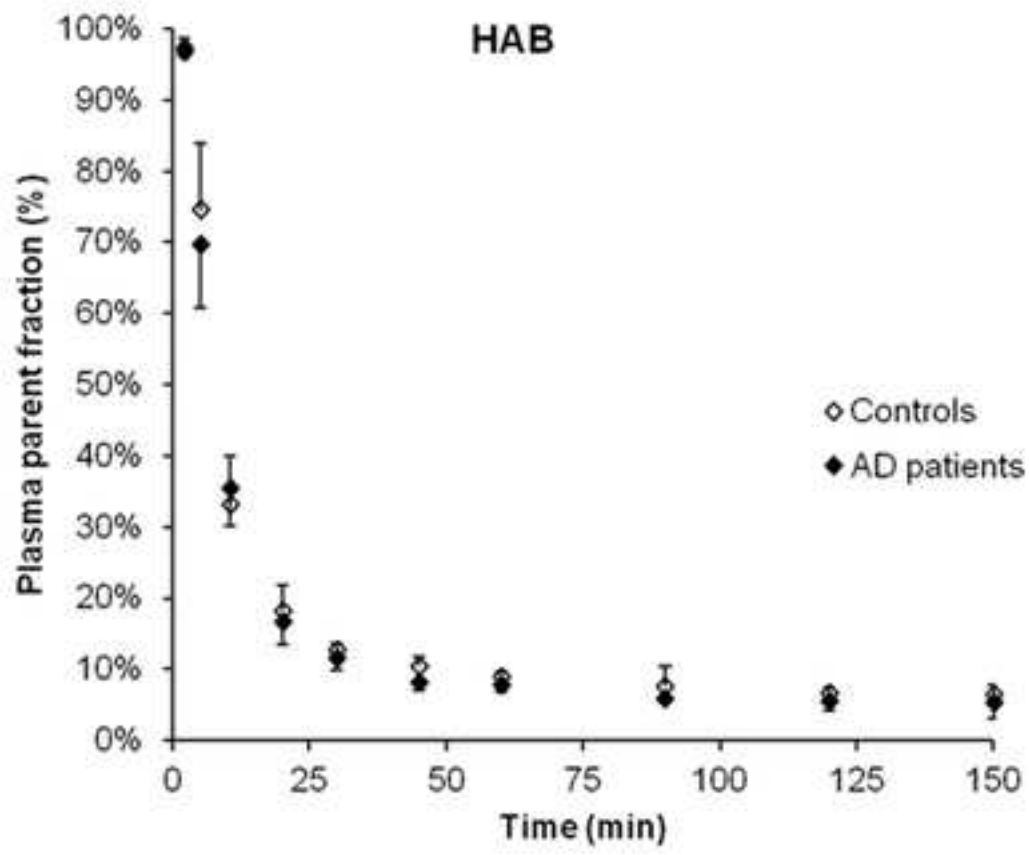
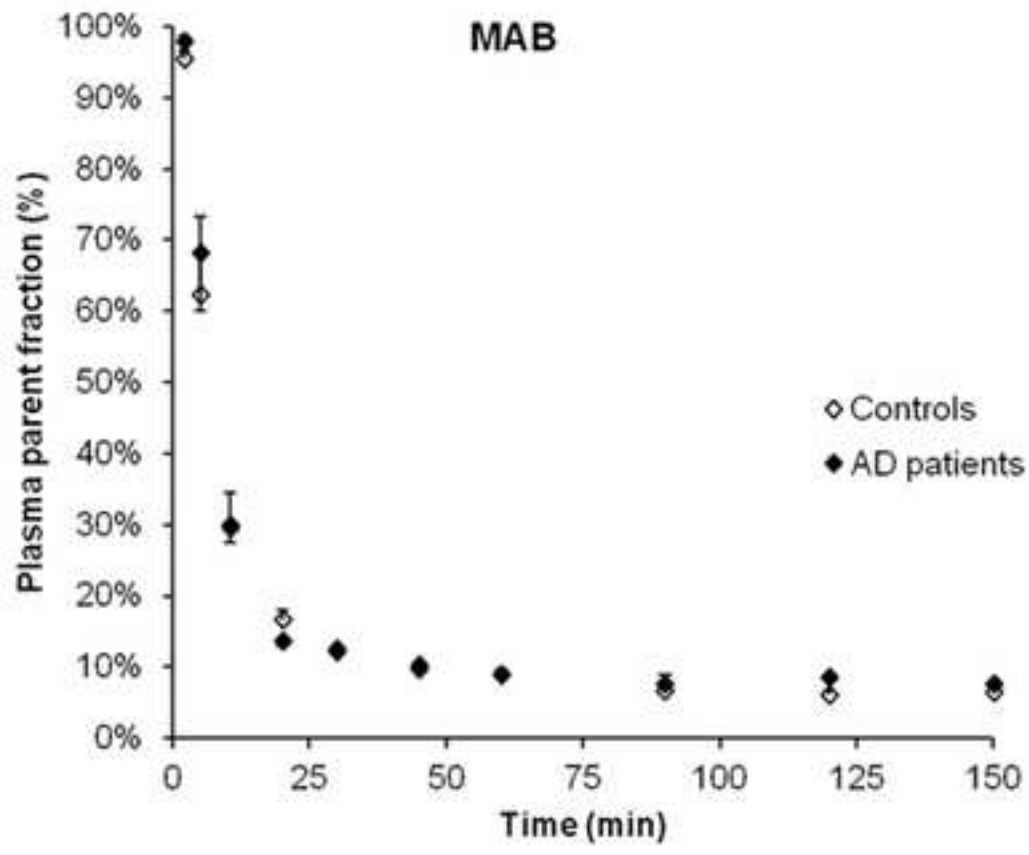


Figure 2
[Click here to download high resolution image](#)

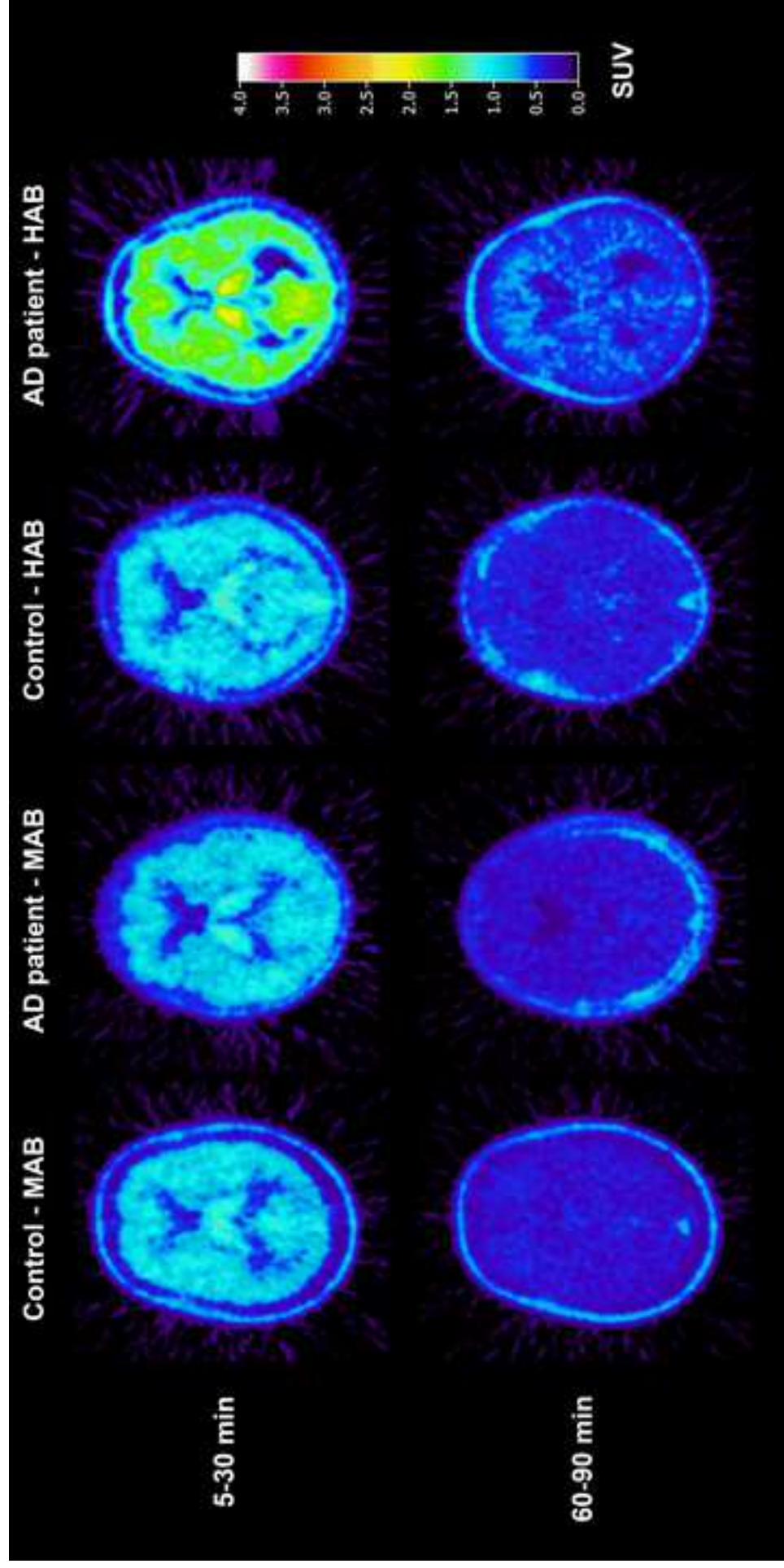


Figure 3
[Click here to download high resolution image](#)

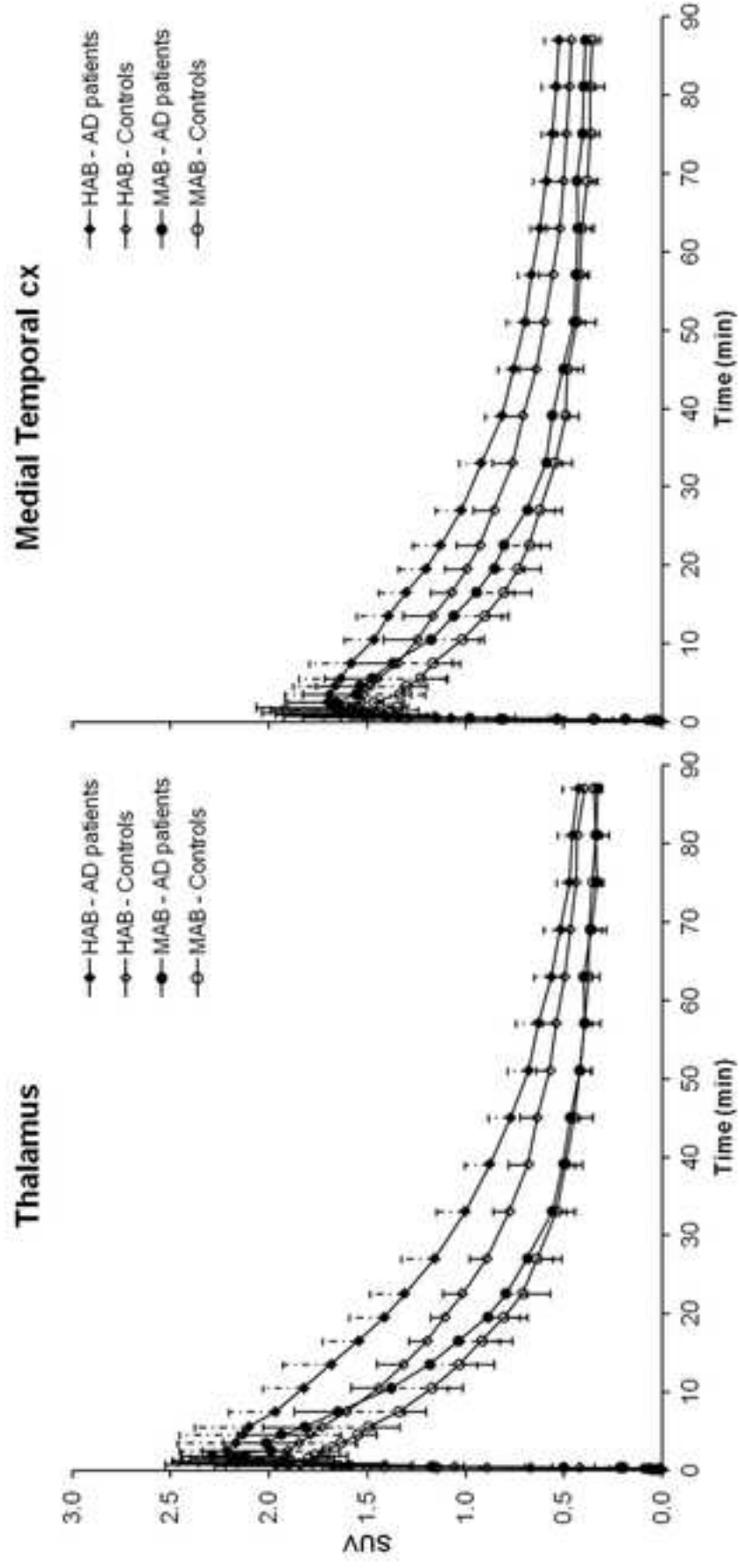


Figure 4

[Click here to download high resolution image](#)

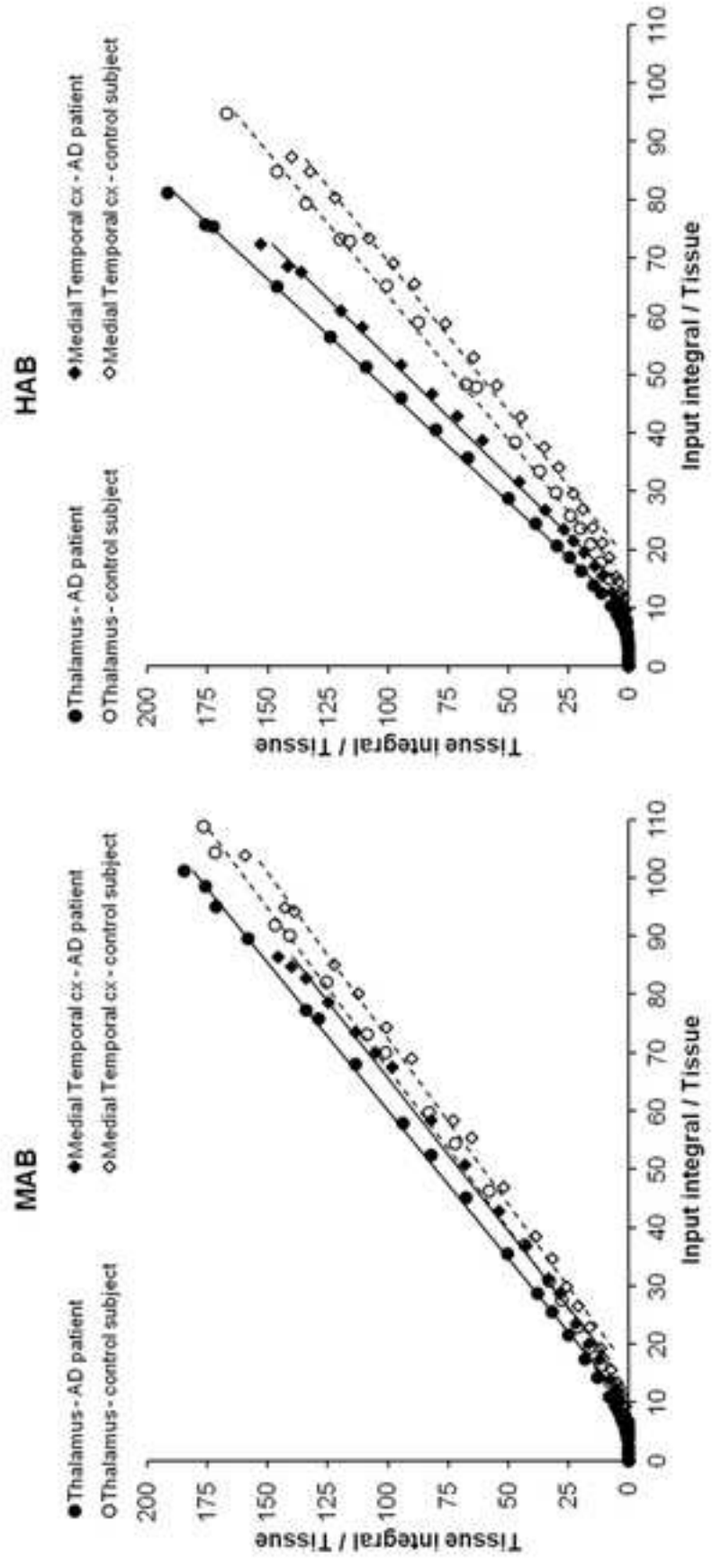
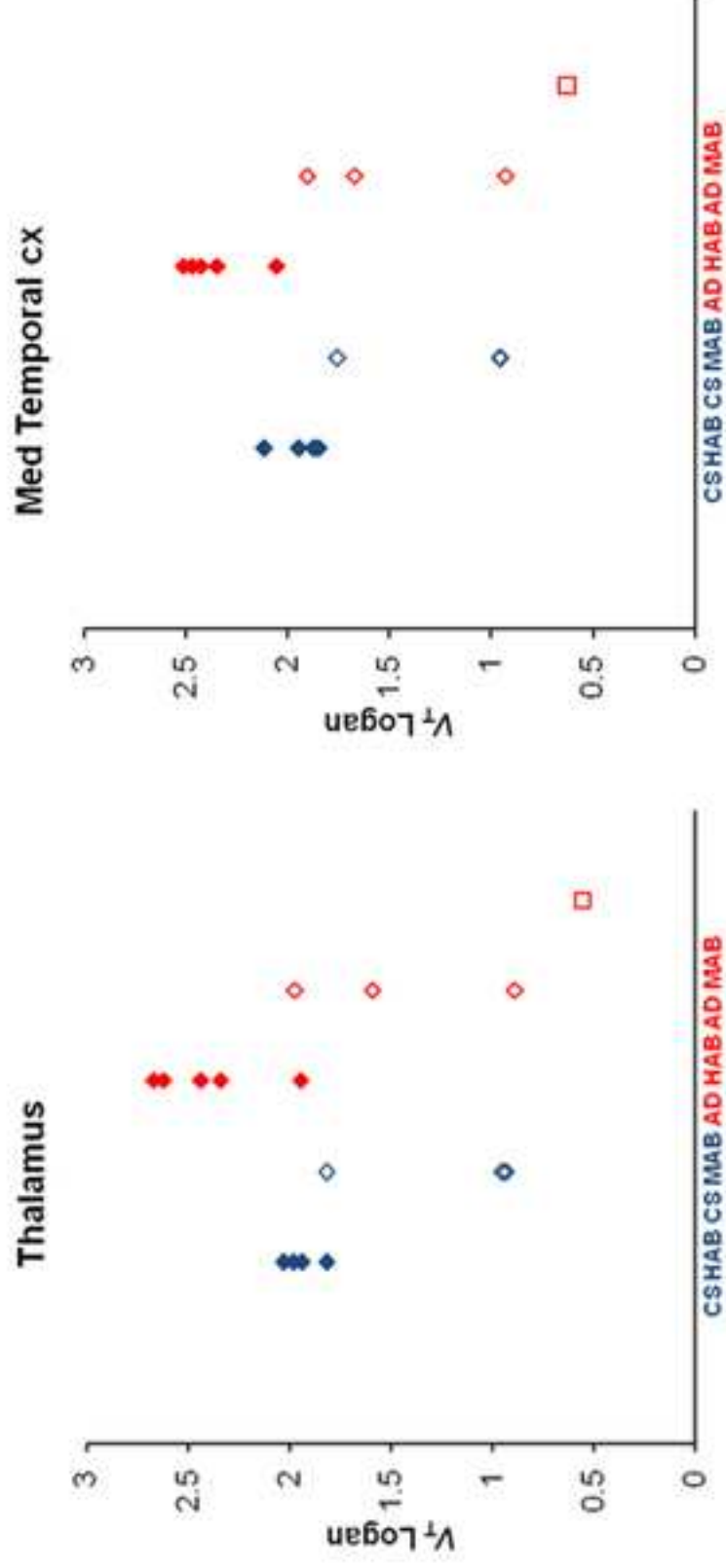


Figure 5

[Click here to download high resolution image](#)



1
2
3 **Positron emission tomography imaging of the 18-kDa Translocator Protein (TSPO) with**
4 **[¹⁸F]FEMPA in Alzheimer's disease patients and control subjects**

5
6
7 Andrea Varrone^{1*}, Vesa Oikonen^{2*}, Anton Forsberg¹, Juho Joutsa², Akihiro Takano¹, Olof
8
9 Solin², Merja Haaparanta-Solin², Sangram Nag¹, Ryuji Nakao¹, Nabil Al-Tawil³, Lisa A.
10
11 Wells⁴, Eugenii A. Rabiner⁴, Ray Valencia⁵, Marcus Schultze-Mosgau⁵, Andrea Thiele⁵, Sonja
12
13 Vollmer⁵, Thomas Dyrks⁵, Lutz Lehman⁵, Tobias Heinrich⁵, Anja Hoffmann⁵, Agneta
14
15 Nordberg⁶, Christer Halldin¹, Juha O. Rinne²

16
17
18 ¹Karolinska Institutet, Department of Clinical Neuroscience, Centre for Psychiatry Research,
19
20 Stockholm, SWEDEN

21
22 ²Turku PET Centre, University of Turku, Turku, FINLAND

23
24 ³Karolinska Trial Alliance, Karolinska University Hospital, Stockholm, SWEDEN

25
26 ⁴Imanova Center for Imaging Sciences, London, UK

27
28 ⁵Bayer Healthcare AG, Berlin, GERMANY

29
30 ⁶Department of Geriatric Medicine, Karolinska University Hospital Huddinge, Stockholm,
31
32 SWEDEN

33
34 *These authors equally contributed to the manuscript

35
36
37 Word count abstract/text: 300/[47834930](#)

38
39 Financial support: Bayer Healthcare, Berlin, Germany; FP7/2007-2013-n° HEALTH-F2-2011-
40
41 278850 (INMIND).

42
43 Address for correspondence:

44
45 Andrea Varrone, MD, PhD

46
47 Karolinska Institutet

48
49 Department of Clinical Neuroscience

1
2
3
4
5
6
7
8
9
10
11
12
13
14
15
16
17
18
19
20
21
22
23
24
25
26
27
28
29
30
31
32
33
34
35
36
37
38
39
40
41
42
43
44
45
46
47
48
49
50
51
52
53
54
55
56
57
58
59
60
61
62
63
64
65

Centre for Psychiatry Research
Karolinska Hospital R5:02
SE-17176 Stockholm, Sweden
E-mail: andrea.varrone@ki.se

1
2
3 **Abstract**
4

5 Imaging of the 18-kDa translocator protein (TSPO) is a potential tool for examining microglia
6 activation and neuroinflammation in early Alzheimer's disease (AD). [¹⁸F]FEMPA is a novel
7 high-affinity, second-generation, TSPO radioligand displaying suitable pharmacokinetic
8 properties in pre-clinical studies. The aims of this study were to assess the quantification of
9 the binding of [¹⁸F]FEMPA to TSPO in AD patients and controls and to investigate whether
10 higher [¹⁸F]FEMPA binding in AD vs. controls could be detected *in vivo*.
11
12

13 **Methods.** Ten AD patients (5M/5F, age 66.9±7.3 y, MMSE 25.5±2.5) and seven controls
14 (3M/4F, age 63.7±7.2 y, MMSE 29.3±1.0) were studied using [¹⁸F]FEMPA at Turku (n=13)
15 and at Karolinska Institutet (n=4). The *in vitro* binding affinity for TSPO was assessed using
16 PBR28 in a competition assay with [³H]PK11195 in 7 controls and 8 AD. Cortical and
17 subcortical regions-of-interest were examined. Quantification was performed using two-tissue
18 compartment model (2TCM) and Logan graphical analysis (GA). The outcome measure was
19 the total distribution volume (V_T). Repeated-measure analysis of variance was used to assess
20 the effect of group or TSPO binding status on V_T .
21
22

23 **Results.** Five AD and 4 controls were high-affinity binders (HABs). Three AD and 3 controls
24 were mixed-affinity binders. V_T estimated with Logan GA correlated significantly with V_T
25 estimated with 2TCM in both controls ($r=0.97$) and AD patients ($r=0.98$) and was selected for
26 the final analysis. In the medial temporal cortex, statistically significant higher V_T ($p=0.044$)
27 in AD vs. controls was found if the TSPO binding status was entered as covariate. If only
28 HABs were included, statistically significant higher V_T in AD patients vs. control subjects
29 ($p<0.05$) was found in the medial and lateral temporal cortex, posterior cingulate, caudate,
30 putamen, thalamus, and cerebellum.
31
32
33
34
35
36
37
38
39
40
41
42
43
44
45
46
47
48
49
50
51
52
53
54
55
56
57
58
59
60
61
62
63
64
65

1
2
3
4
5
6
7
8
9
10
11
12
13
14
15
16
17
18
19
20
21
22
23
24
25
26
27
28
29
30
31
32
33
34
35
36
37
38
39
40
41
42
43
44
45
46
47
48
49
50
51
52
53
54
55
56
57
58
59
60
61
62
63
64
65

Conclusions. [¹⁸F]FEMPA seems to be a suitable radioligand to detect increased TSPO binding in AD if the binding status is taken into account.

Key words. Neuroinflammation, microglia, translocator protein, dementia, Alzheimer

Introduction

Neuroinflammation is a pathological phenomenon characterized by microglia activation and reactive astrocytosis. Neuroinflammatory changes are observed in various neurodegenerative disorders including Alzheimer's disease (AD). Post-mortem studies in AD patients have shown that microglial activation is associated with the presence of amyloid plaques [1][1], suggesting a link between amyloid pathology and neuroinflammation. In vivo imaging of microglial activation can be a useful tool for early detection of neuroinflammation in AD. The 18-kD translocator protein (TSPO) is a mitochondrial protein [2, 3][2, 3] expressed in macrophages [4][4], microglia cells [5][5] and reactive astrocytes [6][6] and is considered a marker of activated microglia and macrophages [7][7]. ((R)-1-(2-chlorophenyl)-*N*-¹¹C-methyl-*N*-(1-methylpropyl)-3-isoquinoline carboxamide ([¹¹C](*R*)-PK11195) was the first TSPO radioligand developed for imaging of activated microglia. The first evidence of increased TSPO binding in AD patients using [¹¹C](*R*)-PK11195 was reported by Cagnin et al. [8][8]. This finding was replicated in a group of 13 AD patients that were also examined with the amyloid radioligand [¹¹C]PIB [9][9]. A large overlap of TSPO binding signal was however observed between controls and patients with AD or with mild cognitive impairment (MCI), using [¹¹C](*R*)-PK11195 [10, 11][10, 11]. It was suggested that either microglia activation in AD is a subtle phenomenon [11][11] or that [¹¹C](*R*)-PK11195 is not enough sensitive to detect in vivo increased microglia activation in AD [10][10].

Several TSPO radioligands with greater affinity than [¹¹C](*R*)-PK11195 have been developed [12][12] and some of them have been used for in vivo imaging of neuroinflammation. Increased TSPO binding in AD and MCI patients compared with controls has been found using the high-affinity radioligand *N*-(2,5-¹¹C-dimethoxybenzyl)-*N*-(5-fluoro-2-phenoxyphenyl)acetamide ([¹¹C]DAA1106) [13, 14][13, 14]. When the ¹⁸F-analog of

1
2
3 DAA1106, *N*-(5-fluoro-2-phenoxyphenyl)-*N*-(2-¹⁸F-fluoroethyl-5-methoxybenzyl)acetamide
4 ([¹⁸F]FEDAA1106) was used, no statistically significant increase of TSPO binding in AD
5 patients could be detected in comparison with controls [15][15]. A large variability of
6
7 outcome measures of [¹⁸F]FEDAA1106 among different subjects was observed [15][15].
8
9

10
11 A major source of variability in TSPO binding is known to be related to the presence of
12 different binding affinity profiles. This property was first demonstrated and fully examined for
13 the high-affinity TSPO radioligand (*N*-{2-(methoxy)phenyl}methyl}-*N*-[4-(phenoxy)-3-
14 pyridinyl]acetamide (PBR28) [16][16], but it was also shown for other second-generation
15 TSPO ligands [17][17]. In the case of [¹¹C]PBR28 it has been demonstrated that the *rs6971*
16 polymorphism of the TSPO gene is responsible for the presence of different binding affinity
17 profiles [18][18]. Subjects can be high- mixed- and low-affinity binders (HABs, MABs,
18 LABs) based on the homozygosity or heterozygosity for the polymorphism. Therefore,
19 imaging of the TSPO using second-generation radioligands should take into account the
20 binding status of the study participants, particularly when different groups of subjects are
21 examined. Recently, increased TSPO binding in amyloid-positive AD patients has been
22 demonstrated using ¹¹C-PBR28 and adjusting for TSPO genotype [19][19].
23
24

25
26
27
28
29
30
31
32
33
34
35
36
37
38
39
40
41
42
43
44
45
46
47
48
49
50
51
52
53
54
55
56
57
58
59
60
61
62
63
64
65

N-{2-[2-(¹⁸F)fluoroethoxy]-5-methoxybenzyl}-N-[2-(4-methoxyphenoxy)pyridine-3-
yl]acetamide ([¹⁸F]FEMPA [CAS 1207345-42-3]) is an aryloxy pyridylamide derivative that is
less lipophilic than [¹⁸F]FEDAA1106, and pre-clinical data in non-human primates showed a
fast elimination from the brain and a better signal-to-noise ratio. Based on these initial pre-
clinical findings suggesting favorable kinetic properties of [¹⁸F]FEMPA, it was decided to
move forward with the characterization of the radioligand in human subjects. [¹⁸F]FEMPA
was considered to be a potential ¹⁸F-labelled TSPO radioligand with similar kinetic properties
(rapid wash-out from the brain and high target-to-background ratio) as the ¹¹C-labelled TSPO

Formatted: Superscript

Formatted: Superscript

Formatted: Superscript

1
2
3
4
5
6
7
8
9
10
11
12
13
14
15
16
17
18
19
20
21
22
23
24
25
26
27
28
29
30
31
32
33
34
35
36
37
38
39
40
41
42
43
44
45
46
47
48
49
50
51
52
53
54
55
56
57
58
59
60
61
62
63
64
65

tracer PBR28. The aims of the present study were therefore to assess the quantification of the in vivo binding of [¹⁸F]FEMPA to TSPO in AD patients and controls and to investigate whether in AD patients increased binding of [¹⁸F]FEMPA to the TSPO could be demonstrated in vivo.

Materials and methods

Subjects

The study was conducted in line with the Helsinki Declaration and approved by FIMEA and the Swedish Medical Products Agency, the local Ethics Committee of the Southwest Hospital District of Finland and of the Stockholm region, and by the Radiation Safety Committee of the Turku Hospital and the Karolinska University Hospital. The study was registered at www.ClinicalTrials.gov (NCT01153607) and included a total of 24 participants. Seventeen of those participants were included in the present study, whereas 7 participants were included in a whole-body dosimetry study that will be reported separately.

Ten AD patients and 7 controls were studied at Turku PET Centre (13 subjects) and at Karolinska Institutet (4 subjects) (Table 1). All subjects gave written informed consent for participation in the study. AD patients were recruited from the University of Turku and from the Karolinska University Hospital, Huddinge. Controls were recruited by local advertisement and from a database at the Karolinska Trial Alliance in Stockholm. All subjects underwent careful clinical and neurological examinations, Mini-Mental State Examination (MMSE), and neuropsychological testing including assessment of memory function. Probable AD was diagnosed according to the clinical criteria of the National Institute of Neurological and Communicative Disorders and Stroke and Alzheimer's Disease and Related Disorders Association (NINCDS-ADRDA) and the criteria of the Diagnostic and Statistical Manual of Mental Disorders (DSM IV). In addition to these criteria, the diagnostic criteria defined by McKahn et al. that include imaging (1998) or CSF and in vivo biomarkers (2003) were used, particularly for those patients showing unimpaired global cognition (MMSE 28, 29 and 30).

The inclusion criterion was mild to moderate disease (MMSE score ≥ 20 and a Clinical Dementia Rating score of 1 or 2). Other forms of dementia (e.g. dementia with Lewy bodies)

Field Code Changed

1
2
3 had to be excluded. Patients were under stable treatment (at least 6 months before the study)
4
5 with cholinesterase inhibitors. Additionally, neither AD patients nor controls were allowed to
6
7 show signs of systemic autoimmune or inflammatory disease. Participants with other current
8
9 treatments acting on the central nervous system (including anti-inflammatory treatments in
10
11 pre-specified time frames) were also excluded in order to avoid interference with the in vivo
12
13 binding of the radioligand.

14 15 *PET experimental procedures*

16
17
18 Details of radiolabelling procedures of [¹⁸F]FEMPA are described in Supplementary
19
20 Appendix 1. Specific radioactivity at time of injection was between 31 and 1343 GBq/μmol.
21
22 The injected radioactivity was 251±16 MBq in control subjects and 251±10 MBq in AD
23
24 patients. The injected mass was 0.68±0.97 (range 0.07-2.55) μg in control subjects and
25
26 0.67±1.16 (range 0.09-3.74) μg in AD patients. There were no significant adverse or clinically
27
28 detectable pharmacologic effects in any of the 17 subjects. No significant changes in vital
29
30 signs or the results of laboratory studies or electrocardiograms were observed.

31 32 33 *PET measurements*

34
35
36 PET measurements were performed with the ECAT EXACT HR+ (Turku PET Center)
37
38 and the ECAT EXACT HR (Karolinska Institutet) systems in two PET sessions. The first PET
39
40 session consisted of a 90-min dynamic acquisition with a series of frames of increasing
41
42 duration (6x5 sec, 3x10 sec, 2x20 sec, 4x60 sec, 6x180 sec, 11x360 sec). The second PET
43
44 session of 30 min was performed between 120 and 150 min after radioligand injection and
45
46 consisted of 5 frames of 360 sec. A transmission scan of 5 min was acquired before each
47
48 dynamic acquisition using three rotating ⁶⁸Ge sources. At Turku, images were reconstructed
49
50 with filtered back projection, a 256x256 matrix, and a pixel size of 1.226x1.226 mm. At
51
52

1
2
3 Karolinska Institutet, images were reconstructed with filtered back projection, with a 2-mm
4 Hanning filter, a zoom factor of 2.17, and a 128x128 matrix. Images were corrected for
5 attenuation and scatter. A NEMA Jaszack phantom with spheres of different diameter and
6 uniform background filled with ¹⁸F-radioactive solution at a ratio of ~4:1 was acquired at both
7 centers under similar experimental conditions and using the standard reconstruction method at
8 each centre. The difference of the recovery coefficient between the two PET systems was
9 9.4% for the spheres and 4.2 for the background, suggesting the possibility to pool the data
10 from the two PET systems.

Formatted: Superscript

11
12
13 Arterial blood sampling was performed using an automated blood sampling system
14 (Allogg AB, Mariefred, Sweden) for the first 10 min and using manual samples thereafter.
15 Samples for metabolite analysis (HPLC, Appendix 1) were taken at 2, 5, 10.5, 20, 30, 45, 60,
16 90, 120, and 150 min.

17 18 19 *Magnetic resonance imaging*

20
21 MRI was performed at Turku University using a Philips Gyroscan Intera 1.5 T Nova
22 Dual scanner (Philips, Best, the Netherlands) and at the Karolinska Institutet using a 1.5-T GE
23 Signa system (GE Healthcare, Milwaukee, WI). MRI scans consisted of a T2-weighted
24 sequence for ruling out pathological changes and a 3-D T1-weighted spoiled gradient recalled
25 (SPGR) sequence for both coregistration with PET and volume-of-interest (VOI) analysis.
26 MRI scans were evaluated for white matter changes according to the Age-Related White
27 Matter Changes (ARWMC) scale [20][20], and exclusion criteria were an ARWMC score of
28 >1 in the basal ganglia and >2 in the subcortical white matter.

29 30 31 *Image analysis*

1
2
3 Image analysis was performed at Turku PET Centre. PET images were coregistered to
4 the T1-weighted MRI using SPM2 (Wellcome Department of Imaging Neuroscience, London,
5 UK). Volumes of interest (VOIs) were delineated using the software Imadeus 1.20 (Forima
6 Inc, Turku, Finland). The following regions were defined: frontal cortex, parietal cortex,
7 lateral and medial temporal cortex, occipital cortex, posterior cingulate cortex, caudate,
8 putamen, thalamus, pons, cerebellum and the subcortical white matter.
9
10
11
12
13
14

15 *TSPO binding status*

16
17
18 The TSPO binding status was measured at Imanova Centre for Imaging Sciences from
19 peripheral blood samples. In two AD patients (AD1 and AD2) the plasma was not available
20 for the binding competition assay. The PBR28 binding status was measured using competition
21 binding assay with ³H-PK11195 on platelet membrane suspension (Supplementary Appendix
22 2). Data were analysed using GraphPad Prism 5.0 Software. One and two site binding models
23 were compared using a sum-of-square *F*-test. In four subjects (CS6, CS7, AD8, and AD9), the
24 binding status was less reliably measured because of low protein concentration in the samples.
25
26
27
28
29
30
31
32

33 *Data analysis*

34
35
36 A preliminary analysis showed that the first PET session was sufficient for
37 quantification of [¹⁸F]FEMPA binding. Therefore, only 90 min of data were used for the final
38 analysis. The radioactivity concentration in the different brain regions was reported as
39 standard uptake value (SUV) and calculated as $SUV = \text{kBq/cm}^3 \div \text{Bq injected} / \text{body weight}$
40 (g). Two parameters were measured to assess the kinetic properties of [¹⁸F]FEMPA: the time
41 to peak uptake (t_{peak}) and the time when the brain radioactivity decreased to 50% of the peak
42 ($t_{\text{half-peak}}$), both expressed in min. The quantification was performed using kinetic and Logan
43 graphical analysis (GA). Kinetic analysis was performed with nonlinear least square (NLS)
44
45
46
47
48
49
50
51
52

1
2
3 fitting and two tissue compartment model (2TCM), with four parameters (K_1 , K_1/k_2 , k_3/k_4 , k_4)
4 and blood volume fitted for each region. The outcome measure was the total distribution
5 volume (V_T). In one subject (AD2), arterial blood sampling was not successful, and this
6 patient was excluded from further analyses. The variability of V_T estimated with 2TCM and
7 Logan GA was calculated as the ratio between the SD over the mean for each brain region and
8 expressed as percentage (coefficient of variance=COV%).

15 *Statistical analysis*

18 Regression analysis was used to assess the agreement between 2TCM and Logan GA in
19 the estimation of V_T . F-test was used to compare the variability of V_T (%COV) estimated with
20 2TCM and Logan GA. Repeated measure analysis of variance (RM-ANOVA) was applied to
21 test the effect of the group (AD patients vs. controls) and TSPO binding status (MAB or
22 HAB) on V_T . Brain region (VOI) was entered as within subject factor, the group as between
23 subject factor and the TSPO binding status as covariate. RM-ANOVA was also applied only
24 to the data from the HABs. In this case, no covariate was entered in the model. As post-hoc
25 analysis, ANOVA was applied to test the differences in V_T between AD patients and controls
26 in different brain regions. Statistical significance was evaluated at $p < 0.05$.

Results

TSPO binding status

Four controls were HABs and 3 were MABs, whereas 5 AD patients were HABs and 3 were MABs (Supplementary Appendix 2). No LABs were observed in either group. The K_i high for the HABs was 2.26 ± 0.18 nM. The K_i high and low for the MABs were 1.93 ± 0.75 nM and 189.8 ± 14.4 nM, respectively.

Radiometabolite analysis

[^{18}F]FEMPA showed rapid metabolism in vivo with <20% of tracer present in plasma 20 min after injection and <10% after 90 min (Figure 1 and Supplementary Figure 1 and 2). There were no statistically significant differences in the parent fraction or in the fraction of metabolites between control subjects and AD patients and between MABs and HABs (Figure 1).

Kinetic properties of [^{18}F]FEMPA

Representative SUV images and mean time-activity curves of [^{18}F]FEMPA are presented in Figures 2 and 3. In each binding group there were no statistically significant differences between controls and AD patients in kinetic parameters based on SUV data (Supplementary Table 1). However, among the AD patients the $t_{\text{half-peak}}$ was significantly lower in MABs than in HABs ($p=0.008$), whereas only a trend was observed in the controls ($p=0.15$).

PET quantification

A preliminary comparison between one tissue compartment model and 2TCM showed that 2TCM provided a better fitting of the data by visual inspection and based on Akaike

1
2
3 Information Criteria, therefore only 2TCM was used in the final analysis of the data
4
5 (Supplementary Figure 3, Supplementary Table 2 and 3). In HABs, V_T values were
6
7 significantly higher ($p<0.05$) in AD patients compared with controls in parietal cortex, lateral
8
9 and medial temporal cortex, posterior cingulate, thalamus and cerebellum.

10
11 Representative Logan plots of [^{18}F]FEMPA are presented in Figure 4. There was a
12
13 statistically significant correlation between V_T estimated with 2TCM and with Logan GA in
14
15 controls ($r=0.97$, $p<0.001$) and AD patients ($r=0.98$, $p<0.001$) across all regions and subjects,
16
17 with values close to the line of identity (Supplementary Figure 4). The mean COV% of V_T
18
19 estimated with Logan GA tended to be lower than the mean COV% of V_T estimated with
20
21 2TCM in AD patients ($p=0.05$, Supplementary Table 4). Logan GA was selected for the final
22
23 analysis of the data, considering the high correlation of V_T between Logan GA and 2TCM and
24
25 the slightly lower COV% of V_T estimated with Logan GA in AD patients.
26

27
28 RM-ANOVA using Logan V_T showed a significant effect of TSPO ($F=17.3$, $p=0.001$)
29
30 and a significant region*TSPO binding status interaction ($F=5.2$, $p=0.004$). The group showed
31
32 only a non-significant trend ($F=3.7$, $p=0.077$). No statistically significant region*group
33
34 interaction was found. However, when only HABs were included in the analysis, a significant
35
36 effect of group ($F=9.2$, $p=0.02$) was observed but no statistically significant region*group
37
38 interaction was found. In all subjects, if the TSPO binding status was entered as covariate, a
39
40 statistically significant difference between groups was found in the medial temporal cortex
41
42 (Table 2). If only the HABs were included, statistically significant differences between groups
43
44 were found in lateral and medial temporal cortex, posterior cingulate, caudate, putamen,
45
46 thalamus and cerebellum (Table 2). In HABs, the V_T values (mean \pm SD) in these regions were
47
48 on average 19.5 \pm 3.0% higher in AD patients as compared with controls, ranging from 15%
49
50
51
52
53
54
55
56
57
58
59
60
61
62
63
64
65

1
2
3 higher in the lateral temporal cortex to 24% in the thalamus (Table 2, Figure 5 and
4
5 Supplementary Figure 5).
6
7
8
9

10 **Discussion**

11
12
13 This study was designed to examine the quantification of the binding to TSPO of the
14 novel radioligand [¹⁸F]FEMPA in controls and AD patients and to evaluate whether increased
15 TSPO binding in AD could be demonstrated in vivo. The primary outcome measure in this
16 study was V_T , estimated using kinetic and Logan GA and the metabolite corrected arterial
17 input function, since no reference region for TSPO is present in the brain. Since a major
18 source of variability in V_T for all second-generation TSPO radioligands is known to come
19 from the *rs6971* polymorphism of the TSPO [18][18], the binding status of the subjects was
20 evaluated using competition assay with ³H-PK11195 and PBR28. In a separate work, the
21 binding properties of FEMPA have been tested on human brain tissue samples, known to
22 belong to different binder subtypes, and it was found that the ratio in affinity between LABs
23 and HABs was approximately 12 (unpublished, data), thus ~4.6 times lower than PBR28.
24
25
26
27
28
29
30
31
32
33
34
35

36 The main finding of this study was that increased in vivo binding of [¹⁸F]FEMPA to
37 TSPO in AD patients could be demonstrated if the binding status of the subjects was taken
38 into account and more specifically if only HABs were included. [¹⁸F]FEMPA appeared to be a
39 suitable radioligand for in vivo TSPO quantification, displaying good brain uptake, fast wash-
40 out from the brain and relatively fast metabolism. V_T estimated using Logan GA was in very
41 good agreement with V_T estimated using 2TCM and showed also lower variability in both
42 controls and AD patients.
43
44
45
46
47
48
49

50
51 *TSPO binding status*
52
53
54
55
56
57
58
59
60
61
62
63
64
65

1
2
3 In this study the TSPO binding status was examined in a competition assay with ³H-
4 PK11195 and PBR28. It is known that this assay provides results in agreement with the
5 analysis of the polymorphism of the TSPO gene [21][21]. The K_i high for the HABs
6 ~~(2.26±0.18 nM)~~ was in good agreement with the K_i value (3.10±5 nM) ~~(3.4±0.5 nM)~~
7 previously reported by Owen et al. [16][16]. The K_i high and low for the MABs ~~(1.93±0.75-~~
8 ~~nM and 189.8±14.4 nM)~~ were also in agreement with the K_i high and low values (4.0±2.4 and
9 313±76.8 nM) previously reported [16][16], although the K_i low for MABs was more in
10 agreement with the K_i low previously reported for LABs (188±15.6 nM) [16][16]. Although
11 in 4 subjects the protein concentration in the assay was low, leading to a reduced signal-to-
12 noise ratio, the V_T for HABs was approximately 2.2 times higher than the V_T for MABs, in
13 agreement with the ratio of V_T between HABs and MABs found across all subjects, which was
14 approximately 1.5. This ratio is also in agreement with the ratio between HABs and MABs
15 reported for ¹¹C-PBR28 [18][18].
16
17
18
19
20
21
22
23
24
25
26
27
28
29

30 *Quantification of [¹⁸F]FEMPA binding to TSPO*

31
32 The fast kinetic properties of [¹⁸F]FEMPA compared with its analog [¹⁸F]FEDAA1106
33 represent a potential advantage for its clinical use. The kinetic analysis showed that the 2TCM
34 was a suitable model for the quantification of [¹⁸F]FEMPA and that V_T estimates obtained
35 with Logan GA were in close agreement with the 2TCM. In this study, we only observed
36 HABs and MABs according to the in vitro binding affinity data. We attempted to estimate the
37 V_T for a LAB, based on the results of the MABs and HABs (Supplementary Appendix 3). The
38 estimated $V_{T\text{LAB}}$ was 0.57±0.08 in controls and 0.74±0.28 in AD patients. Interestingly, this
39 value is similar to the lowest V_T value found in the AD patient that was not analysed for the
40 binding status and that most likely corresponds to a LAB. Assuming that the non-specific
41 binding is similar in HABs, MABs and LABs, and that $V_{ND} < V_T^{\text{LAB}}$, the binding potential
42
43
44
45
46
47
48
49
50
51
52
53
54
55
56
57
58
59
60
61
62
63
64
65

(BP_{ND}) calculated from the distribution volumes ($BP_{ND}=V_T/V_{ND}-1$) can be estimated to be at least ~2 in HABs and ~1 in MABs. Interestingly, the estimated BP_{ND} of [18 F]FEMPA we obtained for HABs and MABs was in agreement with the calculated BP_{ND} for [11 C]PBR28 recently reported by Owen et al. in a blocking study using the TSPO agonist XBD173 [22].

Increased TSPO binding in AD

We observed that in HABs the increase of [18 F]FEMPA binding to the TSPO was between 15% and 24%. These findings are in agreement with previous reports using either [11 C](R)-PK11195 in AD patients (approximately 20-35% increased in cortical binding as compared with controls) (9), [11 C]DAA1106 in MCI (26% increase) and AD patients (18% increase) (13, 14), or [11 C]PBR28 in AD patients (38% increase) (19). Considering the relatively small sample size of this study, statistically significant increased TSPO signal in early AD was detected only after controlling for the TSPO binding status, suggesting the potential of [18 F]FEMPA to detect microglia activation in AD.

Additional considerations

The binding of [11 C]PBR28 to the TSPO has been shown to correlate negatively with the MMSE [19]. We examined the correlation of [18 F]FEMPA mean cortical (frontal, temporal, parietal, and occipital), limbic (medial temporal cortex and posterior cingulate) and sub-cortical (caudate, putamen and thalamus) V_T with MMSE and found a weak, non significant negative correlation (r between -0.37 and -0.41, p -value between 0.12 and 0.17) when combining data from controls and AD patients (data not shown). The lack of statistically significant correlation might be related to the limited sample size and further studies are needed to specifically examine the relationship between TSPO binding of [18 F]FEMPA and cognitive function in AD.

Formatted: Superscript

Formatted: Superscript

Formatted: Font: Italic

Formatted: Subscript

Formatted: Font: Italic

Formatted: Font: Italic

Formatted: Superscript

1
2
3 The analysis of the PET data was conducted using only conventional ROI-based
4 approach. Voxel-based analysis could be useful to identify differences in small areas that can
5 be underestimated by the use of large ROIs. In this study we did not apply voxel-based
6 analysis because of the limited sample size of both groups and to avoid possible false-positive
7 and negative results that can be associated with small samples.

8
9
10
11
12
13
14 The potential application of an ¹⁸F-labelled tracer in the clinical setting could be aided
15 by the use of a simplified acquisition protocol. However, in the case of [¹⁸F]FEMPA, because
16 of the lack of a reference region in the brain the arterial input function data is needed to
17 estimate V_T . We did not observe differences in the parent fraction between AD patients and
18 controls, suggesting that the observed differences in V_T are indeed reflecting differences in the
19 brain distribution of the tracer. Such differences could be detected only by measuring the
20 brain uptake as SUV. We did observe differences in SUV between the two groups, similar to
21 differences in V_T (data not shown), which might suggest that SUV could be used as surrogate
22 outcome measure. However, to validate SUV as potential outcome measure in the clinical
23 setting, additional studies with [¹⁸F]FEMPA in a larger group of AD patients and controls are
24 needed.

Formatted: Superscript

Formatted: Superscript

Formatted: Font: Italic

Formatted: Subscript

Formatted: Font: Italic

Formatted: Subscript

Formatted: Font: Italic

Formatted: Subscript

Formatted: Superscript

Formatted: Font: Italic

36 **Conclusions**

37
38
39 [¹⁸F]FEMPA seems to be a suitable radioligand for in vivo imaging and quantification of
40 TSPO in early AD, provided that the TSPO binding status is determined or by including only
41 HABs. Future studies are needed to confirm these findings in a larger cohort of AD patients.

46 **Acknowledgments**

47
48
49 This study was sponsored by Bayer Healthcare, Berlin, Germany. The work at Turku
50 PET Centre and Karolinska Institutet was supported by the European Union's Seventh

1
2
3
4
5
6
7
8
9
10
11
12
13
14
15
16
17
18
19
20
21
22
23
24
25
26
27
28
29
30
31
32
33
34
35
36
37
38
39
40
41
42
43
44
45
46
47
48
49
50
51
52
53
54
55
56
57
58
59
60
61
62
63
64
65

Framework Programme (FP7/2007-2013) under grant agreement n° HEALTH-F2-2011-278850 (INMIND). The compound [¹⁸F]FEMPA is now part of the portfolio of the Piramal Imaging GmbH, Berlin, Germany. The authors thank the staff of the Turku PET Centre, the Karolinska Institutet PET Centre and the Karolinska University Hospital for technical support.

1
2
3
4
5
6
7
8
9
10
11
12
13
14
15
16
17
18
19
20
21
22
23
24
25
26
27
28
29
30
31
32
33
34
35
36
37
38
39
40
41
42
43
44
45
46
47
48
49

Table 1. Details of Controls and AD patients and their binding status.

Controls/AD patients	Centre	Gender	Age (y)	MMSE	Binding status	Treatment
CS1	Turku	M	66	28	HAB	n.a.
CS2	Turku	F	56	29	MAB	n.a.
CS3	Turku	M	55	30	MAB	n.a.
CS4	Turku	F	69	30	HAB	n.a.
CS5	Turku	F	71	28	HAB	n.a.
CS6	KI	M	58	30	MAB	n.a.
CS7	KI	F	71	30	HAB	n.a.
	Mean±SD	64±7	29.3±1.0			
AD1	Turku	M	74	23	na	Rivastigmine 9.5mg QD
AD2*	Turku	F	56	29	na	Donepezil 10mg QD
AD3	Turku	M	69	28	HAB	Rivastigmine 9.5mg QD
AD4	Turku	M	55	25	MAB	Donepezil 10mg QD
AD5	Turku	F	67	26	HAB	Rivastigmine 9.5mg QD
AD6	Turku	F	76	24	HAB	Donepezil 10mg QD
AD7	Turku	F	67	22	MAB	Donepezil 5mg QD
AD8	KI	F	71	27	HAB	Donepezil 5 mg
AD9	KI	M	61	28	MAB	Galantamine 16 mg
AD10	Turku	M	73	23	HAB	Donepezil 10 mg QD
	Mean±SD	67±7	25.5±2.5†			

*AD2: not analysed because only 10 min of blood data available

†= significantly different from Controls by two-tailed un-paired t-test, $p=0.002$

HAB = High Affinity Binder (9), MAB = Mixed Affinity Binder (6), LAB = Low Affinity Binder (0).

1
2
3
4
5
6
7
8
9
10
11
12
13
14
15
16
17
18
19
20
21
22
23
24
25
26
27
28
29
30
31
32
33
34
35
36
37
38
39
40
41
42
43
44
45
46
47
48
49

Table 2. V_T values of Logan GA in Controls and AD patients (mean \pm SD) with results of ANOVA. The analysis was conducted on all subjects (HABs and MABs) and on the HAB subjects only (4 Controls, 5 AD patients). In the ANOVA conducted on all subjects, the TSPO binding status was included as covariate.

Region	V_T , all subjects		Group	V_T , only HABs		Group
	Controls	AD patients	F (p value)	Controls	AD patients	F (p value)
Frontal cx	1.59 \pm 0.40	1.68 \pm 0.63	1.8 (0.202)	1.85 \pm 0.12	2.12 \pm 0.23	4.4 (0.075)
Parietal cx	1.40 \pm 0.32	1.61 \pm 0.52	4.6 (0.052)	1.61 \pm 0.17	1.86 \pm 0.16	5.2 (0.056)
Lat Temp cx	1.50 \pm 0.35	1.61 \pm 0.55	2.8 (0.122)	1.72 \pm 0.10	1.98 \pm 0.17	7.0 (0.033)
Med Temp cx	1.64 \pm 0.48	1.88 \pm 0.69	5.1 (0.044)	1.95 \pm 0.12	2.36 \pm 0.18	15.2 (0.006)
Occip cx	1.46 \pm 0.35	1.60 \pm 0.52	2.3 (0.154)	1.65 \pm 0.28	1.82 \pm 0.23	1.0 (0.353)
Post Cingulate	1.62 \pm 0.44	1.86 \pm 0.67	4.1 (0.066)	1.91 \pm 0.10	2.30 \pm 0.24	9.1 (0.020)
Caudate	1.25 \pm 0.33	1.35 \pm 0.49	1.9 (0.193)	1.45 \pm 0.05	1.68 \pm 0.19	6.0 (0.045)
Putamen	1.46 \pm 0.44	1.67 \pm 0.64	3.6 (0.080)	1.73 \pm 0.10	2.10 \pm 0.23	8.9 (0.020)
Thalamus	1.64 \pm 0.48	1.89 \pm 0.75	4.1 (0.064)	1.94 \pm 0.09	2.40 \pm 0.29	9.1 (0.019)
Pons	1.70 \pm 0.50	1.92 \pm 0.80	2.8 (0.121)	2.00 \pm 0.15	2.42 \pm 0.35	5.0 (0.060)
Cerebellum	1.43 \pm 0.35	1.61 \pm 0.60	4.2 (0.064)	1.67 \pm 0.06	2.00 \pm 0.24	6.9 (0.034)
White matter	1.44 \pm 0.44	1.61 \pm 0.66	2.4 (0.146)	1.70 \pm 0.14	2.03 \pm 0.33	3.3 (0.111)

1
2
3 **Figure Legend**
4

5 **Figure 1.** Mean plasma parent fraction in mixed-affinity binder (MAB) and high-affinity
6 binder (HAB) in controls and AD patients. The error bars represent 1 SD.
7

8
9
10 **Figure 2.** Representative SUV images of mixed-affinity binders (MAB) and high-affinity
11 binders (HAB). Transaxial slices at the level of the basal ganglia from two control subjects
12 and two AD patients are shown. Frames between 5 and 30 min (top row) and between 60 and
13 90 min (bottom row) were averaged.
14
15
16

17
18
19 **Figure 3.** Mean TACs from mixed-affinity binder (MAB) and high-affinity binder (HAB)
20 Controls and AD patients in thalamus and medial temporal cortex. Error bars represent 1 SD.
21
22

23
24 **Figure 4.** Representative Logan plots of thalamus and medial temporal cortex from mixed-
25 affinity binders (MAB) and high-affinity binders (HAB). Data are from the same control
26 subjects and AD patients displayed in Figure 2.
27
28

29
30 **Figure 5.** Scatter plot of V_T values in control subjects and AD patients (HABs and MABs) for
31 thalamus and medial temporal cortex. The AD patient displayed with the open square was not
32 analysed for TSPO binding.
33
34
35
36
37
38
39
40
41
42
43
44
45
46
47
48
49
50
51
52
53
54
55
56
57
58
59
60
61
62
63
64
65

1
2
3
4
5
6
7
8
9
10
11
12
13
14
15
16
17
18
19
20
21
22
23
24
25
26
27
28
29
30
31
32
33
34
35
36
37
38
39
40
41
42
43
44
45
46
47
48
49
50
51
52
53
54
55
56
57
58
59
60
61
62
63
64
65

Conflict of interest

Ray Valencia, Marcus Schultze-Mosgau, Andrea Thiele, Sonja Vollmer, Thomas Dyrks, Lutz Lehman, Tobias Heinrich, Anja Hoffmann were employed by Bayer Healthcare, Berlin, Germany at the time of the conduction of the study.

1
2
3 **References**

- 4
5 1. ~~Halliday G, Robinson SR, Shepherd C, Kril J. Alzheimer's disease and~~
6 ~~inflammation: a review of cellular and therapeutic mechanisms. Clin Exp Pharmacol Physiol.~~
7 ~~2000;27:1-8.~~
- 8
9
10 2. ~~Rupprecht R, Papadopoulos V, Rammes G, Baghai TC, Fan J, Akula N, et al.~~
11 ~~Translocator protein (18 kDa) (TSPO) as a therapeutic target for neurological and psychiatric~~
12 ~~disorders. Nat Rev Drug Discov. 2010;9:971-88.~~
- 13
14
15 3. ~~Searf AM, Kassiou M. The translocator protein. J Nucl Med. 2011;52:677-80.~~
- 16
17
18 4. ~~Bird JL, Izquierdo-Garcia D, Davies JR, Rudd JH, Probst KC, Figg N, et al.~~
19 ~~Evaluation of translocator protein quantification as a tool for characterising macrophage~~
20 ~~burden in human carotid atherosclerosis. Atherosclerosis. 2010;210:388-91.~~
- 21
22
23 5. ~~Cosenza-Nashat M, Zhao ML, Suh HS, Morgan J, Natividad R, Morgello S, et~~
24 ~~al. Expression of the translocator protein of 18 kDa by microglia, macrophages and astrocytes~~
25 ~~based on immunohistochemical localization in abnormal human brain. Neuropathol Appl~~
26 ~~Neurobiol. 2009;35:306-28.~~
- 27
28
29 6. ~~Kuhlmann AC, Guilarte TR. Cellular and subcellular localization of peripheral~~
30 ~~benzodiazepine receptors after trimethyltin neurotoxicity. J Neurochem. 2000;74:1694-704.~~
- 31
32
33 7. ~~Venneti S, Lopresti BJ, Wiley CA. Molecular imaging of~~
34 ~~microglia/macrophages in the brain. Glia. 2013;61:10-23.~~
- 35
36
37 8. ~~Cagnin A, Brooks DJ, Kennedy AM, Gunn RN, Myers R, Turkheimer FE, et al.~~
38 ~~In vivo measurement of activated microglia in dementia. Lancet. 2001;358:461-7.~~
- 39
40
41 9. ~~Edison P, Archer HA, Gerhard A, Hinz R, Pavese N, Turkheimer FE, et al.~~
42 ~~Microglia, amyloid, and cognition in Alzheimer's disease: An [¹¹C](R)PK11195-PET and~~
43 ~~[¹¹C]PIB-PET study. Neurobiol Dis. 2008;32:412-9.~~
- 44
45
46
47
48
49
50
51
52
53
54
55
56
57
58
59
60
61
62
63
64
65

10. ~~Wiley CA, Lopresti BJ, Venneri S, Price J, Klunk WE, DeKosky ST, et al. Carbon 11 labeled Pittsburgh Compound B and carbon 11 labeled (R)-PK11195 positron emission tomographic imaging in Alzheimer disease. Arch Neurol. 2009;66:60-7.~~
11. ~~Schuitmaker A, Kropholler MA, Boellaard R, van der Flier WM, Kloet RW, van der Doef TF, et al. Microglial activation in Alzheimer's disease: an (R)-[(1)(1)C]PK11195-positron emission tomography study. Neurobiol Aging. 2013;34:128-36.~~
12. ~~Dolle F, Luus C, Reynolds A, Kassiou M. Radiolabelled molecules for imaging the translocator protein (18 kDa) using positron emission tomography. Curr Med Chem. 2009;16:2899-923.~~
13. ~~Yasuno F, Ota M, Kosaka J, Ito H, Higuchi M, Doronbekov TK, et al. Increased binding of peripheral benzodiazepine receptor in Alzheimer's disease measured by positron emission tomography with [11C]DAA1106. Biol Psychiatry. 2008;64:835-41.~~
14. ~~Yasuno F, Kosaka J, Ota M, Higuchi M, Ito H, Fujimura Y, et al. Increased binding of peripheral benzodiazepine receptor in mild cognitive impairment dementia converters measured by positron emission tomography with [(1)(1)C]DAA1106. Psychiatry Res. 2012;203:67-74.~~
15. ~~Varrone A, Mattsson P, Forsberg A, Takano A, Nag S, Gulyas B, et al. In vivo imaging of the 18 kDa translocator protein (TSPO) with [18F]FEDAA1106 and PET does not show increased binding in Alzheimer's disease patients. Eur J Nucl Med Mol Imaging. 2013;40:921-31.~~
16. ~~Owen DR, Howell OW, Tang SP, Wells LA, Bennacef I, Bergstrom M, et al. Two binding sites for [3H]PBR28 in human brain: implications for TSPO PET imaging of neuroinflammation. J Cereb Blood Flow Metab. 2010;30:1608-18.~~

Formatted: English (U.S.)

- 1
2
3 ~~17. Owen DR, Gunn RN, Rabiner EA, Bennacef I, Fujita M, Kreisl WC, et al.~~
4 ~~Mixed affinity binding in humans with 18 kDa translocator protein ligands. J Nucl Med.~~
5 ~~2011;52:24-32.~~
6
7
8
9 ~~18. Owen DR, Yeo AJ, Gunn RN, Song K, Wadsworth G, Lewis A, et al. An 18-kDa~~
10 ~~translocator protein (TSPO) polymorphism explains differences in binding affinity of the PET~~
11 ~~radioligand PBR28. J Cereb Blood Flow Metab. 2012;32:1-5.~~
12
13
14
15 ~~19. Kreisl WC, Lyoo CH, McGwier M, Snow J, Jenko KJ, Kimura N, et al. In vivo~~
16 ~~radioligand binding to translocator protein correlates with severity of Alzheimer's disease.~~
17 ~~Brain. 2013;136:2228-38.~~
18
19
20
21 ~~20. Wahlund LO, Barkhof F, Fazekas F, Bronge L, Augustin M, Sjogren M, et al. A~~
22 ~~new rating scale for age-related white matter changes applicable to MRI and CT. Stroke.~~
23 ~~2001;32:1318-22.~~
24
25
26
27 ~~21. Kreisl WC, Jenko KJ, Hines CS, Lyoo CH, Corona W, Morse CL, et al. A~~
28 ~~genetic polymorphism for translocator protein 18 kDa affects both in vitro and in vivo~~
29 ~~radioligand binding in human brain to this putative biomarker of neuroinflammation. J Cereb~~
30 ~~Blood Flow Metab. 2013;33:53-8.~~
31
32
33
34
35
36
37
38
39
40 1. Wyss-Coray T, Rogers J. Inflammation in Alzheimer disease—a brief review of
41 the basic science and clinical literature. Cold Spring Harb Perspect Med. 2012;2:a006346.
42
43
44 2. Rupprecht R, Papadopoulos V, Rammes G, Baghai TC, Fan J, Akula N, et al.
45 Translocator protein (18 kDa) (TSPO) as a therapeutic target for neurological and psychiatric
46 disorders. Nat Rev Drug Discov. 2010;9:971-88.
47
48
49
50 3. Scarf AM, Kassiou M. The translocator protein. J Nucl Med. 2011;52:677-80.
51
52
53
54
55
56
57
58
59
60
61
62
63
64
65

Formatted: English (U.S.)

Formatted: Font: Times New Roman, 12 pt

Formatted: Indent: Left: 0", First line: 0",
Line spacing: Double

- 1
2
3 4. Bird JL, Izquierdo-Garcia D, Davies JR, Rudd JH, Probst KC, Figg N, et al.
4
5 Evaluation of translocator protein quantification as a tool for characterising macrophage
6
7 burden in human carotid atherosclerosis. Atherosclerosis. 2010;210:388-91.
- 8
9 5. Cosenza-Nashat M, Zhao ML, Suh HS, Morgan J, Natividad R, Morgello S, et
10
11 al. Expression of the translocator protein of 18 kDa by microglia, macrophages and astrocytes
12
13 based on immunohistochemical localization in abnormal human brain. Neuropathol Appl
14
15 Neurobiol. 2009;35:306-28.
- 16
17 6. Kuhlmann AC, Guilarte TR. Cellular and subcellular localization of peripheral
18
19 benzodiazepine receptors after trimethyltin neurotoxicity. J Neurochem. 2000;74:1694-704.
- 20
21 7. Venneti S, Lopresti BJ, Wiley CA. Molecular imaging of
22
23 microglia/macrophages in the brain. Glia. 2012.
- 24
25 8. Cagnin A, Brooks DJ, Kennedy AM, Gunn RN, Myers R, Turkheimer FE, et al.
26
27 In-vivo measurement of activated microglia in dementia. Lancet. 2001;358:461-7.
- 28
29 9. Edison P, Archer HA, Gerhard A, Hinz R, Pavese N, Turkheimer FE, et al.
30
31 Microglia, amyloid, and cognition in Alzheimer's disease: An [11C](R)PK11195-PET and
32
33 [11C]PIB-PET study. Neurobiol Dis. 2008;32:412-9.
- 34
35 10. Wiley CA, Lopresti BJ, Venneti S, Price J, Klunk WE, DeKosky ST, et al.
36
37 Carbon 11-labeled Pittsburgh Compound B and carbon 11-labeled (R)-PK11195 positron
38
39 emission tomographic imaging in Alzheimer disease. Arch Neurol. 2009;66:60-7.
- 40
41 11. Schuitemaker A, Kropholler MA, Boellaard R, van der Flier WM, Kloet RW,
42
43 van der Doef TF, et al. Microglial activation in Alzheimer's disease: an (R)-[(1)(1)C]PK11195
44
45 positron emission tomography study. Neurobiol Aging. 2013;34:128-36.
- 46
47 12. Dolle F, Luus C, Reynolds A, Kassiou M. Radiolabelled molecules for imaging
48
49 the translocator protein (18 kDa) using positron emission tomography. Curr Med Chem.
50
51 2009;16:2899-923.

- 1
2
3 13. Yasuno F, Ota M, Kosaka J, Ito H, Higuchi M, Doronbekov TK, et al. Increased
4 binding of peripheral benzodiazepine receptor in Alzheimer's disease measured by positron
5 emission tomography with [11C]DAA1106. Biol Psychiatry. 2008;64:835-41.
6
7
8
9 14. Yasuno F, Kosaka J, Ota M, Higuchi M, Ito H, Fujimura Y, et al. Increased
10 binding of peripheral benzodiazepine receptor in mild cognitive impairment-dementia
11 converters measured by positron emission tomography with [(1)(1)C]DAA1106. Psychiatry
12 Res. 2012;203:67-74.
13
14
15
16
17 15. Varrone A, Mattsson P, Forsberg A, Takano A, Nag S, Gulyas B, et al. In vivo
18 imaging of the 18-kDa translocator protein (TSPO) with [18F]FEDAA1106 and PET does not
19 show increased binding in Alzheimer's disease patients. Eur J Nucl Med Mol Imaging.
20 2013;40:921-31.
21
22
23
24
25 16. Owen DR, Howell OW, Tang SP, Wells LA, Bennacef I, Bergstrom M, et al.
26 Two binding sites for [3H]PBR28 in human brain: implications for TSPO PET imaging of
27 neuroinflammation. J Cereb Blood Flow Metab. 2010;30:1608-18.
28
29
30
31 17. Owen DR, Gunn RN, Rabiner EA, Bennacef I, Fujita M, Kreisl WC, et al.
32 Mixed-affinity binding in humans with 18-kDa translocator protein ligands. J Nucl Med.
33 2011;52:24-32.
34
35
36
37 18. Owen DR, Yeo AJ, Gunn RN, Song K, Wadsworth G, Lewis A, et al. An 18-kDa
38 translocator protein (TSPO) polymorphism explains differences in binding affinity of the PET
39 radioligand PBR28. J Cereb Blood Flow Metab. 2012;32:1-5.
40
41
42
43 19. Kreisl WC, Lyoo CH, McGwier M, Snow J, Jenko KJ, Kimura N, et al. In vivo
44 radioligand binding to translocator protein correlates with severity of Alzheimer's disease.
45 Brain. 2013;136:2228-38.
46
47
48
49
50
51
52
53
54
55
56
57
58
59
60
61
62
63
64
65

1
2
3
4
5
6
7
8
9
10
11
12
13
14
15
16
17
18
19
20
21
22
23
24
25
26
27
28
29
30
31
32
33
34
35
36
37
38
39
40
41
42
43
44
45
46
47
48
49
50
51
52
53
54
55
56
57
58
59
60
61
62
63
64
65

20. Wahlund LO, Barkhof F, Fazekas F, Bronge L, Augustin M, Sjogren M, et al. A new rating scale for age-related white matter changes applicable to MRI and CT. Stroke. 2001;32:1318-22.

21. Kreisl WC, Jenko KJ, Hines CS, Lyoo CH, Corona W, Morse CL, et al. A genetic polymorphism for translocator protein 18 kDa affects both in vitro and in vivo radioligand binding in human brain to this putative biomarker of neuroinflammation. J Cereb Blood Flow Metab. 2013;33:53-8.

22. Owen DR, Guo Q, Kalk NJ, Colasanti A, Kalogiannopoulou D, Dimber R, et al. Determination of [(11)C]PBR28 binding potential in vivo: a first human TSPO blocking study. J Cereb Blood Flow Metab. 2014;34:989-94.

Formatted: Line spacing: Double

Supplementary Figures

[Click here to download Supplementary Material: Supplementary Figures FEMPA manuscript 20140523.docx](#)

Supplementary Tables

[Click here to download Supplementary Material: Supplementary Tables FEMPA manuscript 20140523.docx](#)